Information to the editor

We are pleased to present a revised manuscript entitled “Explicit aerosol-cloud interactions in the Dutch Atmospheric Large-Eddy Simulation model DALES4.1-M7”.

The manuscript was revised according to the response to the reviewers’ comments. Major changes to the documents include:

(i) Rearrangement of the document structure and the inclusion of the appendix into the main text (new Sect. 3.1.2) (*Note that this causes some errors in the marked-up version as latexdiff double counts some removed/added Section numbers*).
(ii) A more elaborate discussion of the model’s capabilities (i.e. omitted processes and simplifications) and its position among other models in the introduction.
(iii) We tuned down the comparison of model outcome to observations and conclusions drawn from this.
(iv) Results from new simulations for KAPPA, SAT0.2, SAT1.0 and PN using a correct volume-mean average of aerosol characteristics.
(v) A more elaborate discussion of the cloud characteristics (Sect. 3.2.1) to accompany the discussion of the differences in aerosol characteristics in Sect. 3.2.3.
(vi) Inclusion of missing references mentioned by the reviewers.

Besides the revisions following from the reviewers’ comments, we made some minor improvements that correct grammatical errors and improves readability. However, these additional changes are limited to single sentences. With these changes, we believe that the manuscript greatly improved and is now more complete. We are confident that we meet the requested standard for publication in GMD.

On behalf of all co-authors,
Marco de Bruine

Response to anonymous referee 1

September 10, 2019

Marco de Bruine et al.

First of all, we would like to thank the reviewer for the careful reading of our manuscript. His/her comments greatly improved the quality of our manuscript, including a better paper structure. Point-by-point replies to the comments are provided below.

1 Simulation resolution and length

Comment 1

A major concern that I would like to highlight is the limitation of the discussion of sample simulations to a single LES resolution, notably a relatively coarse one for a shallow cumulus case. In the 2011 study of Matheou et al. (doi:10.1175/2011MWR3599.1) it was shown that for the RICO simulation setup used in the present paper, even significantly finer grids and larger domains were not enough to achieve convergence in terms of cloud characteristics (see also Sato et al. 2018, doi:10.1029/2018MS001285). While, arguably, such analysis and discussion is not directly related to the scope of the manuscript, it would be of great value for potential users of the developed aerosol module. Moreover, having the limitations of the resolution in mind, and given the absence of convergence tests in the paper, I strongly encourage the authors to critically revisit all parts of the paper commenting on the match with observations.

Response The other reviewer shared this concern of directly comparing model outcome to observations because of the reasons mentioned by the reviewer. We acknowledge these arguments and revisit all parts of the paper commenting on the match with observations.

Changes In the revised manuscript we will focus the discussion in Sect 5.1 on the behaviour of the different simulations and will not draw conclusions based on direct comparison of observations and model outcome. We would still like to keep the observations as a background against which the different simulation set-ups behave. We will also include a statement about the current lack of convergence tests.

Comment 2

Similar concern applies to the length of the simulation. The original RICO setup featured 24 hour simulations, of which several first hours were treated as spin-up, while output result for model intercomparison was carried out using the last four hours of simulation only. In the present paper, 6-hour long simulations are presented (and the conclusions section enumerating the main findings of the study, comments on processes with multi-day timescales). It is essential to point out this difference, provide the reason for shortening the simulations, and comment on it.

Response The reason we use 6-hour long simulations (with the first 3 hours as spin-up excluded from the analysis) is that we are interested in the evolution of a certain aerosol population within a cloud field. We do not simulate emission of new aerosol during the simulations. In a 24-hour long simulation with substantial wash-out by precipitation but no sources would deplete the aerosol population to unrealistically low levels. In our 6-hour simulations we already lose 20-25% of the aerosol mass.

In the Figures of the model output for the RICO LES intercomparison by Van Zanten et al. (2011) as found on http://projects.knmi.nl/rico/ (last visited: 3 September 2019). We see that metrics like LWP and cloud fraction are more or less stable after 3-4 hours. Therefore, we expect that if we would have a sustained aerosol population in a longer simulation, the results would not be substantially different.

Changes We will add additional information on the choice for 6-hour simulations and expectations of how this would influence the results.

Comment 3

How does the intensive precipitation in the second half of the first hour of the RICO case affects the budget of remaining aerosol, and hence how different are the conditions in which clouds form here with respect to those found in models with infinite CCN reservoir? Please discuss.

Response There is indeed substantial wash-out by the initial burst of precipitation during the spin-up of the simulation. As shown in the figure below, 90.7 and 94.4% of the initial budget remains for the KAPPA and PN simulations respectively. At the end of the simulations this decreases to 76.7 and 79.0% for KAPPA and PN.

Our BASE and BASE30 simulations are examples of a model that implicitly assumes an infinite CCN reservoir that results in clouds with a certain Nc and we describe their results in Sect. 5.1. The ultimate goal for this model is to have a fully coupled simulation which includes emissions. However, in this initial paper, our case remains academic and we highlight the sensitivity of the processing of aerosol to the activation scheme.

Changes In the revised manuscript we will address removal of aerosol and the impact on the simulated microphysics.

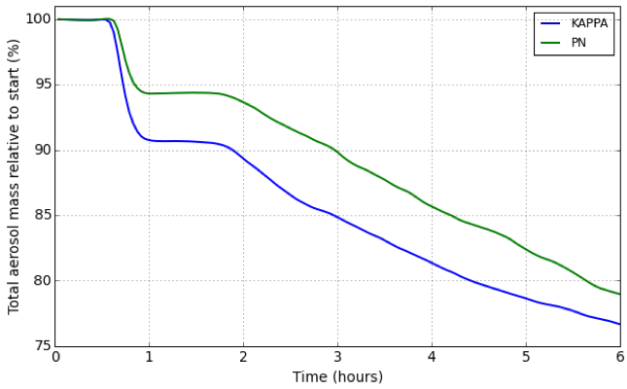

Figure 1: Remaining aerosol budget in the lowest 3 km of the domain relative to the initialisation for the KAPPA and PN simulations.

2 Aerosol processing nomenclature and background information

Comment 4

Aerosol-cloud interaction, as a main theme of the manuscript, is always stated in singular form (i.e., interaction, not interactions). First, in general plural would sounds better in my opinion.

Response & Changes We will follow this suggestion and use the plural form "aerosol-cloud interactions" in the revised manuscript.

Comment 5

Second, it would be worth to elaborate in the paper on the different kinds of interactions, also those beyond the processes covered in DALES-M7. It is striking that aerosol distribution changes through aqueous-phase oxidation are not mentioned in the paper, the mention of chemistry in the penultimate sentence is unclear. Please comment on it and clearly position the capabilities of the introduced model among other available aerosol-cloud interactions modelling frameworks; see, e.g., Ovchinnikov and Easter 2010 (doi:10.1029/2009JD012816) and Jaruga et al. (doi:10.5194/gmd-11-3623-2018) and references therein. Aerosol nucleation processes are also reported to be influenced by clouds (e.g., Wehner et al. 2015, doi:10.5194/acp-15-11701-2015).

Response & Changes We agree, and in the revised manuscript we will add a more elaborate description of the different aerosol-cloud interactions in the introduction, aqueous-phase chemistry in particular. Moreover, in Section 3 we will clarify which of the processes are included in our framework and which are not yet implemented.

Comment 6

On a related note, while the authors claim "resolving most of the turbulence" (worth rephrasing), there is little discussion on how it affects the modelled collisions among aerosol, cloud and precipitation particles - worth mentioning.

Response We agree with the reviewer and add a description of how the resolution in the model compares to the scales involved in particle-level processes like collisions.

Changes In the revised manuscript we rephrased the sentence "resolving most of the turbulence" in response one of the technical comments to page 11, line 14. However, we will add another statement that highlights that although LES is usually considered as a high-resolution simulation, both the spatial resolution of 10m and the temporal resolution of 1s are still too coarse to actually simulate the processes on particle-level for which one would need DNS on the Kolmogorov length-scale of 1mm. These processes therefore remain parameterized in LES.

Comment 7

In general, perhaps putting together a summary of omitted/largely-simplified processes would be a good idea (in-cloud activation, aerosol sedimentation, influence of turbulence on collisions, chemistry, etc)?

Response & Changes As stated in the response to comment 5, we will add a summary of what processes are covered in DALES-M7 and which are not.

Comment 8

Please also make sure it is clear what "explicit" means in different contexts in the paper. In principle, it should be clear (also to readers from neighbouring domains or those focused on largely different scales) what the opposite "implicit" would mean.

Response The meaning of explicit in this paper is "not parameterized", making parameterized the opposite. We acknowledge that by using the term explicit in a manuscript describing numerical methods there is a risk to confuse this with explicit/implicit methods for model integration.

Changes In the revised manuscript, the first mention of explicit aerosol calculation will include an explanation of the opposite being: 'parameterized'. P3, line 12-13 will be adjusted as: "This also allows for explicit calculation of aerosol activation based on the characteristics of the aerosol population, instead of using a parameterization based on i.e. updraft velocity."

Comment 9

Could “free aerosol” when referring to out-of-cloud-or-rain-shafts aerosol be named somehow differently? Ambient aerosol?

Response We used the term ‘free aerosol’ to indicate all aerosol not incorporated in (or captured by, hence the term ‘free’) cloud and rain droplets. This includes for example interstitial aerosol in clouds or aerosol in the path of falling precipitation. In our opinion, the term ‘ambient aerosol’ implies that the aerosol is unaffected by cloud processes in any way, which is not the way we intended to use this term here.

3 Statements calling for references

Comment 10

p6/l4-5: “...cloud and rain droplet modes do not have a lognormal shape...”, see: Clark 1976 (doi:10.1175/1520-0469(1976)0332.0.CO;2) and Feingold and Levin 1986 (doi:10.1175/1520-0450(1986)0252.0.CO;2)

Response What we meant to say here is that in our model, the assumed distribution for the cloud and raindrop size distributions does not need to have a lognormal shape, but can be different. We did not intend to state here that cloud and rain size distributions are not lognormal, which then indeed would need a reference.

Changes In the revised manuscript, we changed the associated text to be more clear and not imply a certain hydrometeor size distribution: “...cloud and rain droplet modes do not necessarily need to have a lognormal shape...”

Comment 11

p10/l11: “but the measurements were fitted to a bimodal lognormal dist.” ? in which work?

Response We based this statement on information from van Zanten et al. (2011) Section 2.2.3 elaborating on the input of models that require an aerosol size distribution.

Changes In the revised manuscript we add the reference and a one-line description: “The aerosol size distribution was measured on aircraft flight RF12, and the measurements were fitted to a bimodal lognormal distribution of aerosols with uniform composition, assuming characteristics of ammonium-bisulfate (see van Zanten et al. (2011), their Sect 2.2.3), despite the marine nature of the environment.”

Comment 12

- p11/l7: "corresponds to the actual observed mean values" ? which day, which aircraft, which sensor, which sampling rate, what kind of analysis, which paper...
- p12/l1: "which is in accordance with observations" ? ditto
- p12/l22: "campaign in-situ observations show values" ? ditto

Response All three statements refer to the observations in Fig. 8 in van Zanten et al. (2011) and Fig. 2 in our manuscript. These measurements are an aggregate of 1 Hz FFSSP measurements on flights RF06-RF12 with the NCAR C-130 aircraft. We will better specify these details and make clear this is the data we refer to in the remainder of the section.

Changes We will change the opening of Sect. 5.1 describing this:

"To evaluate the modelled cloud characteristics produced in the different simulations we follow the analysis of vanZanten et al. (2011). Domain-averaged cloud characteristics are shown in Fig. 3, which is constructed to resemble Fig. 8 in vanZanten et al. (2011). Similar to their work we use an aggregate of 1 Hz FFSSP measurements on flights RF06-RF12 with the C-130 aircraft (Rauber et al., 2006). Cloud characteristics are filtered using the condition qc > 0.01 g kg^{-1}, while rain characteristics use the condition qr > 0.001 g kg^{-1}."

4 Paper structure

Comment 13

Several suggestions and comments to the paper structure:

- Section 3.1 is introduced, but there is no 3.2
- Section 5 "Results" should be somehow linked with the setup (as these are not general results)
- Appendix material fits well into the simulation setup section

Response & Changes We will adopt the suggested structure for the paper, which fixes the unnecessary section depth in Section 3. It also clarifies the fact that we discuss the differences between model simulations and cannot directly compare to observation because of model limitations. Lastly, since the description of the simulation set-up is not too long it indeed fits in the main body of the text and we would not have to include an extra short summary of this as we do in Section 4 of the manuscript now.

Comment 14

Code availability section does not need a number (format as acknowledgements)

Response Adjusted.

5 Code availability

Comment 15

In which branch of DALES github repo one can find the code of DALES-M7?

Response Currently, DALES-M7 is not on the DALES github repository. Instead, everything can be found at the link stated in the code availability section: http://doi.org/10.5281/zenodo.3241356. DALES-M7 is based on the 4.1 branch, which also is the one used for the BASE and BASE30 simulations in this work. This line of development of DALES is currently in progress and still an unfinished research line. After completion, we intend to merge this branch into the main DALES repository (version 4.2).

Comment 16

Is M7 an external dependency or was it incorporated into (or reimplemented?) DALES codebase?

Response It is incorporated in the DALES code base.

Comment 17

What is the license of M7? Is it compatible with DALES?s GPL? Which version of M7 was used/incorporated/reimplemented?

Response There is no GPL defined for M7. Moreover, in this work we only implemented the aerosol representation used by M7. We excluded the dynamic processes of M7, such as nucleation, coagulation and condensation. This will, however, be part of future development of the model.

6 Minor or technical comments

Comment 18

p1/l4: "The feedback of ACI on the aerosol population remains relatively understudied" ? within the abstract, please concentrate on describing the contents of the paper, and not motivation.

Response & Changes In the revised manuscript we wemoved the following sentences containing motivation of this work: "These models combine a spatial resolution high enough to resolve cloud structures with domain sizes large enough to simulate macroscale dynamics and feedback between clouds. However, most research on ACI using LES simulations is

focused on changes in cloud characteristics. The feedback of ACI on the aerosol population remains relatively understudied."

Comment 19

p1/l18-19: please clarify if "larger" refers to size or mass

Response The aerosol size comparison in the last part of the abstract refers to aerosol size (i.e. radius).

Changes Revised manuscript is adjusted to explicitly mentions this: "Analysis of typical aerosol size associated with the different microphysical processes shows that aerosols resuspended by cloud evaporation have a radius that is only 5 to 10% larger than the originally activated aerosols. In contrast, aerosols released by evaporating precipitation are an order of magnitude larger".

Comment 20

p2/l10: "missing atmospheric context" ? please rephrase

Response Adjusted

Changes Sentence in revised manuscript changed to: "...process-based small-scale simulations (e.g. Roelofs, 1992) describe the microphysical processes in high detail, but cannot model the effect of aerosol-cloud interactions on the macroscale thermodynamics and structure of a cloud."

Comment 21

p2/l28: given the paper discusses aerosol-cloud interactions, mentioning also 2D-bin (e.g., Lebo and Seinfeld 2011, doi:10.5194/acp-11-12297-2011) and particle-based methods (e.g., Grabowski et al 2019, doi:10.1175/BAMS-D-18-0005.1) would be apt

Response Indeed, the 'traditional' choice of bin vs. bulk is complemented by particle-based methods like the libcloudph++ by Arabas et al. (2015) or the similar 'superdroplet' method (Riechelmann et al., 2014; Hoffmann et al., 2019). We will also add a reference to the overview paper of Grabowski et al., 2019) as it is a very good illustration of the current status of modelling aerosols and clouds in LES. The extensive 2D-bin method by Lebo & Seinfeld (2011) deserves a mention here as well.

Changes In the revised manuscript we will add references to these methods in the text to inform the reader of these alternative numerical frameworks to study aerosol-cloud interactions.

Comment 22

p3/l3-4: recent advances in representing aerosol in LES are not limited to these two works! please be more comprehensive or rephrase

Response We aimed here to elaborate on LES models that include aerosol frameworks with the focus on multiple aerosol species and/or (aqueous-phase) chemistry.

Changes We will rephrase this paragraph in the revised manuscript to better specify that we focus on aerosol modules in LES simulations including multiple aerosol species. We added Jaruga and Pawlowska (2018) to the discussion as their extension to the libcloudph++ library opens up a range of possibilities to include and interactively calculate multiple aerosol species.

Comment 23

p6/l13-17: unlike in a basic single-particle model as κ-Köhler, activation in clouds happens on populations of particles and with complex supersaturation dynamics related to small-scale fluctuations and drop-growth feedback, please acknowledge what is simplified when just considering a critical supersaturation

Response We indeed acknowledge that by using a direct calculation based on κ-Köhler and using a fixed value for supersaturation leaves out the competition for moisture between non-activated aerosol and existing droplets.

Moreover, by directly translating supersaturation to particle activation, we implicitly assume that the equilibration time of the droplets is instantaneous or at least considerably shorter than the model timestep. This might lead to an overestimation of activated droplets as some particles would activate at a certain supersaturation but did not have enough time to grow to the critical radius yet. This would be better captured by a numerical framework that directly calculates the condensational growth.

Changes We will add this discussion after the description of the activation routine, to the paragraph on page 7, line 12 where we discuss the supersaturation.

Comment 24

p7/l12: please clarify if this is peak or equilibrium in-cloud supersaturation

Response As discussed for the previous comment, in our model we assume that aerosols/droplets equilibrate instantaneously with the supersaturation of the environment. This implies that there is no difference between the two. However, in the KAPPA activation scheme we only activate once and assume all subsequent water surplus condenses on the cloud droplets, so this value would refer to the supersaturation maximum at the cloud base.

Comment 25

p8/l7: first mention of KAPPA, not introduced as an acronym before, please define

Response We remove the reference to the KAPPA simulation here, as this part of the text does not yet refer to the exact simulations performed in this work, but to the activation scheme in general.

Changes Changed sentence to: To avoid this 'runaway activation' in the κ-Köhler-based scheme, activation in a cloudy grid cell is allowed only once.

We also changed PN in this paragraph to PN15 for consistency as we refer to the complete work by Pousse-Nottelmann et al. (2015) here, not the simulation.

Comment 26

p9/l6: final $\rightarrow$ last

Response Adjusted

Comment 27

p9/l11: add "and" before "is calculated"

Response Adjusted

Comment 28

p9/l22:"their Eq. 4" $\rightarrow$ "Eq. 4 therein"

Response Adjusted

Comment 29

p10/l18: being over an ocean is not the point, the point is from where the wind blows and how far from the sources it is

Response Agreed, we specified why the dominance of sea salt aerosol is to be expected here.

Changes Sentence change to: "The aerosol population mainly consists of sea salt particles, as expected for this ocean region with trade winds blowing from the open ocean."

Comment 30

p10/l22: shouldn't the concentrations be expressed in the units of mg^{-1} (to reduce variation from density changes)

Response One of the main figures in our manuscript is Fig 1, which is made to resemble Fig. 8 in Van Zanten et al. (2011). Here, the values are expressed per unit volume. For consistency between figures and values stated in the text we opted to use the units of cm^{-3} here as well.

Comment 31

p11/l14 "beautifully display the richness"... please refrain from vague statements

Response Agreed.

Changes Text adjusted to be more to-the-point and precise: "These cross-sections display the internal variability within the LES model domain that results from the high spatial resolution."

Comment 32

p12/l8: "at left" $\rightarrow$ "at the left"

Response Adjusted

Comment 33

p14/l22: "mighty" $\rightarrow$ "might"

Response Adjusted

Comment 34

p16/l15: perhaps worth commenting on how in-cloud activation was modelled (or neglected)

Response This paragraph is thoroughly revised. Reviewer 2 commented that the difference in cloud processing between PN and KAPPA required more explanation. This manuscript is adjusted to include a description of cloud microphysics in Sect 5.1 and refer to this in Sect 5.2 which will include the difference in activation between the two simulations. For a full description see the response to comment 8 of reviewer 2.

Comment 35

p19/l13: are 4 significant digits needed? p20/l5: ditto

Response & Changes Accuracy of all radii mentioned in paragraph 5.2.2 and Table 5 reduced to 1 nm.

Comment 36

References: please be consistent in using journal name abbreviations vs. full journal names

Response & Changes All journal names now abbreviated using Caltech Library Services (www.library.caltech.edu/reference/abbreviations)

Response to anonymous referee 2

September 10, 2019

Marco de Bruine et al.

First of all, we would like to thank the reviewer for his/her comments and the careful reading of our manuscript. There are several main points made, which will be addressed below.

1 General comments

Comment 1

Aerosol-cloud interaction (ACI) is a rather general term, so quite often this could be replaced by a more specific term. For example, "The feedback of ACI on the aerosol population" (page 1, line 4) could be just "The impact of cloud processing on the aerosol population" and the same term could be used also here "Whether ACI increases or decreases the average aerosol size" (page 1, line 16). Please check the whole manuscript.

Response We agree with the reviewer that the general term ACI should be replaced by a more specific description of the processes in play whenever possible. This complements the comment of the other reviewer stating that ACI is a collection of many different processes.

Changes In the revised manuscript we replace instances with a general reference to ACI by a more direct description of the processes we address.

Comment 2

Using the saturation adjustment method (diagnostic cloud water) and assuming a fixed value for supersaturation when calculating cloud activation are significant approximations. Their effects should be at least explained here instead of investigating these in the future (page 7, line 13). Can you really examine aerosol-cloud interactions without explicitly modeling aerosol condensational growth and subsequent cloud activation (prognostic cloud water)? What is the added value of detailed aerosol chemical composition when cloud activation is so much simplified?

Response The long-term goal for DALES is to create a 'virtual lab' to simulate the atmosphere with as few assumptions as possible. We intend to build a model that can study links

between pollution, atmospheric chemistry (including aqueous chemistry) and clouds. The first step towards this goal is the inclusion of an aerosol representation that fits in this framework. This requires a scheme capable of simulating multiple aerosol species. Therefore, we chose to implement an aerosol module following the framework of M7 (Vignati et al., 2014). This comes at the cost of a limited numerical description of condensational growth and activation of cloud droplets, since a chemically-resolving bin scheme would be computationally too demanding.

We agree that by using a fixed value for the supersaturation, the model misses an important feedback between supersaturation and aerosol activation. For this reason, we included sensitivity runs with different values for S as well as a different activation parameterization (Pousse-Nottelman et al., 2015) as a comparison.

Changes In the revised manuscript we will directly address this instead of stating it will be investigated in the future.

The paragraph at the end of Section 3.1.1 (starting at page 7, line 11) is changed accordingly: "As stated above, DALES uses an 'all-or-nothing' cloud water adjustment in which cloud liquid water qc is a diagnostic variable. Therefore, we use a fixed value of supersaturation (S = 0.4%) representative for the simulated case (Derksen et al., 2009). Moreover, the use of a multi-species aerosol scheme comes at the cost of a limited numerical description of condensational growth and subsequent activation. Including both would be computationally too demanding. As a result, the model thus does not capture the competition for moisture between particles (aerosols and cloud droplets) or the role of supersaturation in this process. To asses impact of changing supersaturation on the cloud characteristics in our simulations, we will perform sensitivity simulations with different values of S. Although fixing the value of S is still an approximation, it does allow for an interactive calculation of cloud droplet number concentration based on simulated aerosol."

Regarding the choice for a multi-species aerosol scheme, we address this in the introduction (page 3, line 13-15). However, in the revised manuscript we highlight this again at the beginning of Sect 3 (page 4, line 25) with the following adaptation: "This framework allows for the simulation of an external mixture of multiple aerosol species. In future development, this will be coupled to atmospheric chemistry, including aqueous-phase chemistry. It also allows for the investigation of differences in how cloud processing influences different aerosol species. By using M7, cloud activation can be based on fundamental . . . "

Comment 3

Why did the "runaway activation" (page 8, line 7) were allowed only for the PN activation scheme? For me this looks like a possible reason for the observation that aerosol fluxes for activation (and cloud evaporation) are 12-13 times larger for PN simulations compared with those from KAPPA simulation. This difference is later used as an explanation for several other differences between simulation results. If the difference between activation schemes is related to a technical/numerical reason, then it should be considered as a bug and fixed.

Response The term 'repeated activation' in this work describes activation of new cloud drops in a cloudy gridcel already containing cloud droplets. This repeated activation is prohibited for the k-Kohler scheme, because the modal representation keeps pushing aerosol mass and number to a size above the activation threshold, so there is no mechanism to limit the activation due to numerical diffusion. Without this limit virtually all aerosol would be activated, leading to erroneously high cloud droplet numbers. We termed this process 'runaway activation'.

The PN activation scheme, however, is fundamentally different and uses other mechanisms to limit unrealistic high cloud droplet numbers. The newly activated cloud droplets $\partial N_c \backslash \partial t$ in this scheme are calculated following Eq. (2) in Pousse-Nottelmann et al (2015):

$$\frac{\partial N_c}{\partial t} = \max \left\{ \frac{1}{\Delta t} \left[\left(\frac{w N^t_{>35}}{w + \alpha N^t_{>35}} \right)^{1.27} - N_c^{t-1} \right], 0 \right\} \tag{1}$$

With w the updraft vertical velocity, Δt the length of the timestep, N_c^{t-1} the number of cloud droplets present, $N^t_{>35}$ the number concentration of soluble/mixed aerosol particles larger than 35 nm and $\alpha = 0.023$ cm^4 s^{-1} an empirically derived constant.

By including updraft velocity w and the existing cloud droplet number N_c^{t-1}, this formulation does include competition for moisture between condensation on existing droplets and activation of new particles. However, the strongest limitation of this formulation is found in the prefactor of 0.1. This prefactor was determined in Zubler et al. (2011a) by comparison of their model outcome against satellite data with respect to the cloud droplet effective radius. The combination of this prefactor and the subtraction of N_c^{t-1} poses such a strong limitation on aerosol activation that 'runaway activation' is not occurring in the PN scheme.

The figure below shows vertical profiles of aerosol activation in terms of aerosol/cloud number. The profiles are normalized individually for each simulation to the maximum of the vertical profile. Note that overall activation in the PN simulation is 12-13 times stronger , as can be inferred from Table 3 and 4 in the paper. However, the vertical distribution of activation in both simulations is similar with a peak near cloud base. Activation above cloud base drops off slightly faster for caused by its dependence on updraft velocity. We therefore conclude that both activation schemes are reasonable and lead to realistic cloud simulations, albeit with widely different aerosol evaporation/activation cycles.

Why the aerosol flux associated with activation and cloud evaporation is so much higher is explained in the reply to the related comment 8.

Summarizing, we deliberately test two valid but fundamentally different cloud-activation schemes to highlight the sensitivity of cloud microphysics to this choice.

Changes In the revised manuscript we will add the above-mentioned formula which is central in the PN scheme and we will better describe why the PN scheme can allow 'repeated activation' without leading to 'runaway activation'.

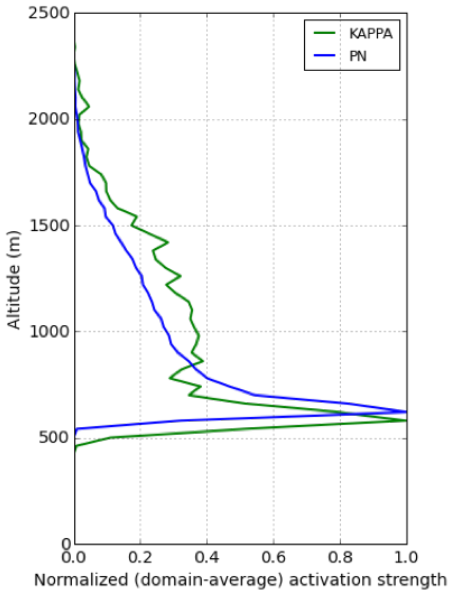

Figure 1: Vertical profile of domain-average aerosol mass-flux to in-cloud aerosol for the KAPPA and PN simulations.

Comment 4

Validating simulations against observations is not as straightforward as expected in this work (e.g. page 10, line 2). LES inputs (aerosol size distributions and composition, atmospheric variables, etc.) are not fully synchronized with the cloud and rain observations, so one-to-one comparison is not fair. I would recommend reformulating/removing all such direct comparisons.

Response We agree with the reviewer's comment that direct comparison of model results and observations is problematic. However, we still believe that the observations of cloud characteristics are useful to be included as a qualitative validation in terms of order of magnitude.

Changes Stimulated also by the comments of both reviewers, we will discuss the results in the revised manuscript mainly in terms of model behaviour and sensitivity, and stick to a more academic approach.

2 Specific comments

Comment 5

P7, Eq. 5: This equation is not valid for hygroscopicity parameter, because some species-specific hygroscopicity parameters are zeros. Did you really used this equation (and how)? This equation can give unrealistic hygroscopicity parameter values (divide by zero) and in that case all calculations should be updated. The correct way to calculate the mode mean hygroscopicity parameters is volume fraction weighted average.

Response We thank the reviewer for pointing out this error in the source code of the model. The mentioned equation (5) was applied, while species with the addition that occurrences of $\kappa = 0$ were left out of the summation preventing division by zero. Nevertheless, the equation is incorrect and will be replaced by the volume-mean average as:

$$\varphi_k = \frac{\sum_i V_i \varphi_i}{\sum_i V_i}, V_i = \frac{m_{i,k}}{\rho_i} \tag{2}$$

For a mode mean aerosol density ρ_k, equation (5) does hold as the occurrences of ρ_i in the numerator cancel out.

$$\rho_k = \frac{\sum_i V_i \rho_i}{\sum_i V_i} = \frac{\sum_i \frac{m_{i,k}}{\rho_i} \varphi_i}{\sum_i \frac{m_{i,k}}{\rho_i}} = \frac{\sum_i m_{i,k}}{\sum_i m_{i,k}/\rho_i} \tag{3}$$

The resulting equation was reused by replacing ρ by κ, for which this cancellation obviously does not happen.

Fortunately, the simulations with the corrected mode mean hygroscopicity only show minor differences. There is only a small differences between the volume and mass-mean average hygroscopicity due to the dominance of sea salt aerosol in the ACS and COS modes. Likewise, the main species in the AIS mode are sulfate (SO4) and organics (POM) which have a similar density (1841 and 1800 kg m^{-3} for SO4 and POM respectively). So in the AIS mode, the mass and volume-mean are comparable as well.

Changes New simulations will be performed using the correct calculation of the volume-mean. The revised manuscript will be updated with the results and figures from the corrected simulations. These modifications are minor and do not affect the results or interpretation.

Comment 6

P12, L27: Maybe the above-mentioned possible bug in hygroscopicity parameter could explain why KAPPA simulations produce much lower cloud droplet number concentration (CDNC) compared with that from the PN simulation? Many other explanations are based on this difference in CDNC (e.g. page 14, line 15-), so a clear explanation is required in any case.
Also, why the interactively calculated CDNCs are so low compared with the available aerosol concentration, and why CDNC seems to be independent of the selected cloud supersaturation? Why does CDNC from the PN simulation decrease with altitude?

Response New simulations were performed using the corrected calculation of the mode volume-mean hygroscopicity parameter. As noted above, the error in the calculation did not cause substantial differences in the cloud characteristics.

The low CDNC in the KAPPA simulation are the direct result of only allowing activation once. As soon as clouds are present in a grid cell new in-cloud activation is prohibited to avoid the 'run-away activation' discussed above. The activated aerosols here are distributed over the whole cloud, which leads to low CDNC without extra in-cloud activation. The changes in S between 0.2 and 1.0% do not change this heavy dilution of CDNC. In the PN simulation, the formulation of activation also severely limits how much of the available aerosol is activated as discussed in the general comment concerning the 'runaway activation'. Both simulations show a decrease of CDNC with altitude as most activation takes place near cloud base.

Changes In the revised manuscript, we will discuss the ratio between aerosol concentration and CDNC and the decrease with altitude for CDNC as mentioned above.

Comment 7

P14, L30 "None of the simulations scores best on all metrics ...": direct comparison of observations and LES simulations is not that simple, but if observations were considered as the truth, would the new KAPPA framework be far from best? Although diagnostic cloud water is accurately predicted, it fails to predict cloud droplet number.

Response The comparison to the observation will be given much less weight in the revised version of the manuscript. However, we still would not argue that the KAPPA framework is far from the best, because that would imply that correctly simulating CDNC is more important than the other metrics.

Changes In the revised manuscript we focus the discussion on how the model outcome changes due to different assumptions and parameterizations and refrain from making statements based on direct comparison with observations. We will highlight that it is difficult to improve all the cloud metrics as follows from the outcome of the different aerosol activation schemes.

Comment 8

P16, L13: Aerosol fluxes for activation (and cloud evaporation) are 12-13 times larger in PN simulation compared with those in KAPPA simulation. The given explanation is based on different autoconversion strengths so that in the KAPPA simulation a larger fraction of cloud water becomes rain before evaporation and is therefore not counted as cloud evaporation, right? If this is the reason, then why cloud-to-rain conversion process strengths are so similar? At least for me, this looks more like a bug than a physically realistic process (see the related general comment). Because meteorology is similar for both PN and KAPPA simulations, there is no physical reason for the large difference between cloud activation fluxes.

Response This paragraph was thoroughly revised. Importantly, the statement: "...the same cloud water is distributed over more but smaller cloud droplets" was incorrect and removed. We are convinced however that the large differences between the two simulations (KAPPA PN) are not caused by a bug. Our conviction is based on two arguments: (1) the meteorological differences which are shown below, and (2) the fundamentally different approach to activation in the two schemes, which allows a higher Nc in the PN scheme than the KAPPA scheme.

Fig 3 panel (b) indicates that the clouds in the PN simulation hold more water than in the KAPPA simulation. By only showing conditional sampled cloud characteristics, the differences between the KAPPA and PN were somewhat hidden. To better illustrate the differences between the simulations, we refer to the figures below. In the leftmost 2 panels, we see that the domain-average cloud water is substantially higher in PN compared to KAPPA (up to +250%). This higher domain-average water load is not only the result of the increased liquid water content in individual clouds as follows from Fig 3, panel (b) in the manuscript. In the rightmost 2 panels, we show that the cloud cover in PN is higher as well. Moreover, by combining Fig 3, panel (d) with data from Tables 3 & 4 we observe that these clouds produce similar amounts of precipitation at the surface and consequently re-evaporate more water.

In conclusion, the PN simulation does produce more clouds, containing more water, but leads to a similar amount of precipitation reaching the surface. These extra clouds thus dissipate and re-evaporate more water back to the atmosphere. This, in combination with activation in the PN simulation leads to the substantially higher aerosol fluxes in the clouds.

Changes In the revised manuscript we will summarize this overview of the difference in meteorology in Section 5.1 and refer to it when discussing the aerosol microphysics in Section 5.2.

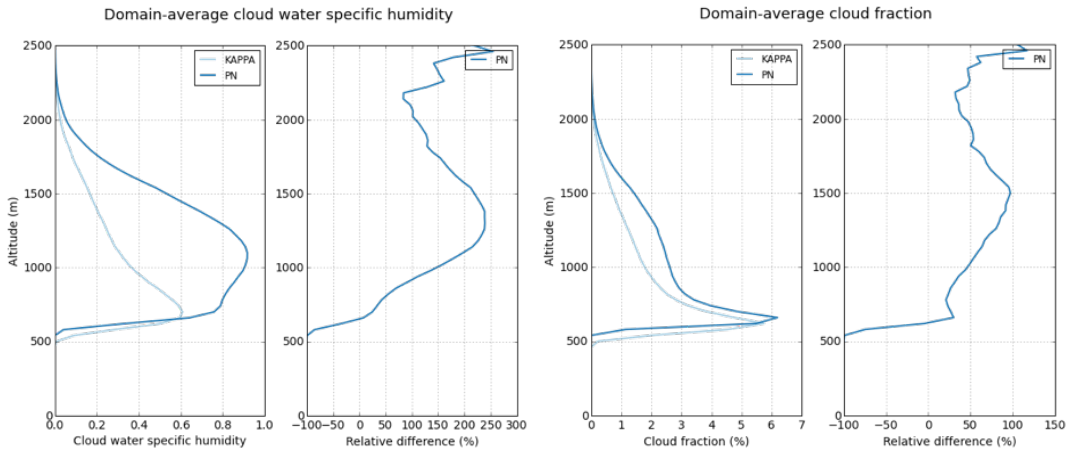

Figure 2: Vertical profile of domain-average (left) cloud liquid water specific humidity and (right) cloud fraction for the KAPPA and PN simulations.

Comment 9

P18, L32-: Average median radius of activated aerosols are different for the KAPPA and PN simulations, and the explanation is related to "stronger cycling of aerosol through the clouds in the PN simulation". What about the effect of supersaturation? It is fixed (0.4%) for KAPPA, but depends on updraft velocity for PN. Lower supersaturation in the PN case could explain the difference in median radius.

Response Nc is higher in the PN simulation than in the KAPPA simulation. This implies that a larger fraction of the aerosols activate. Since both schemes assume that activation of the aerosols progresses from large to small, the higher Nc in the PN simulation goes together with the activation of more small aerosols.

The combination of a higher Nc and a larger average in-cloud aerosol size can therefore not be caused by a lower (effective) supersaturation, and must be the result of the changes of the aerosol distribution by cloud processing.

3 Technical corrections

Comment 10

P1, L3: "feedback between clouds"?

Response & Changes Description made more specific as follows:

These models have a spatial resolution high enough to resolve clouds and associated microphysics. This is combined with domain sizes large enough to simulate macroscale dynamics and mesoscale cloud structures.

Comment 11

P1, L10: "in this pristine ocean environment virtually all aerosols enter" - not all aerosols, but those that activate, right?

Response The purpose of this sentence is to point out that the aerosol (mass) in the cloud droplets is the result of activation. We agree that "in the cloud (phase)" can be understood differently as "in the cloud". This can then imply both activated and interstitial aerosol which is not what we intended to say here.

Changes In the revised manuscript, the sentence is changed so that it is emphasized that we mean the aerosol mass in cloud droplets:

"We find that in this pristine ocean environment virtually all aerosol mass in the cloud droplets is the result of the activation process, while in-cloud scavenging is relatively inefficient."

Comment 12

P2, L17: "which influence further ACI"

Response & Changes In the revised manuscript, this general reference to ACI by a more detailed description as follows:

"Moreover, processing of the aerosol population by one cloud influences the microphysical processes in subsequent clouds. For example, when one cloud depletes the aerosol population by wash out, this might lead to larger clouds droplets in the subsequent cloud formed on the depleted aerosol population. The might lead to faster rain formation and an even further depletion of the aerosol population. This underlines the non-linear character of the interaction between aerosols and clouds and the need to simultaneously simulate the clouds and the aerosol population."

Comment 13

P2, L25: Please clarify "bulk" and "numerical" methods.

Response & Changes Changed text to exclude specific terms like 'bulk' that refer to the way models represent cloud and/or aerosols. This is elaborated upon in the next paragraph.

Sentence change to: "Although methods based on a fixed cloud droplet number, or fixed (infinite) ambient aerosol concentration are almost completely replaced by methods that do consider the aerosol size distribution in a prognostic way. Aerosol composition, however, is often assumed to be uniform."

Comment 14

P2, L33: There is also an ECHAM version with SALSA microphysics.

Response & Changes The reason for including a reference to ECHAM here is to point to models using M7. There indeed is a version of ECHAM with SALSA, but to our knowledge, M7 is still the default microphysics scheme, even in the most recent cycle of the 'ECHAM family' ECHAM-HAMMOZ.

Comment 15

P2, L34: Why "However" here?

Response & Changes To emphasize that the fixed distribution shape is the simplification that is made to achieve the previously mentioned computational efficiency.

Comment 16

P5, L14: "of the originating free aerosol mode"

Response & Changes Sentences are rearranged to clarify cause and effect:

"This modal approach leads to the implicit assumption that the in-hydrometeor aerosol mass is assumed homogeneously distributed across the cloud or rain drop distributions, i.e. aerosol concentrations do not change with hydrometeor size. As a result, size (and mass) information of the originating free aerosol mode is lost once aerosols are incorporated in cloud and raindrops."

Comment 17

P6, L19: S is saturation ratio, right?

Response Correct.

Changes In the revised manuscript, we will highlight this in the description of Eq. (1), but opt to keep using the term supersaturation in the main body of the text.

Comment 18

P11, Fig. 2: The unit of sea salt mass concentration is more likely micro than milligrams per cubic meter. Also, would it be possible to separate clouds and precipitation or otherwise indicate cloud base height to the vertical cross section?

Response & Changes The unit is corrected in the revised manuscript (μg m^{-3}). Cloud (outline) and rain (hatching) liquid water is now indicated separately in the figure as shown below.

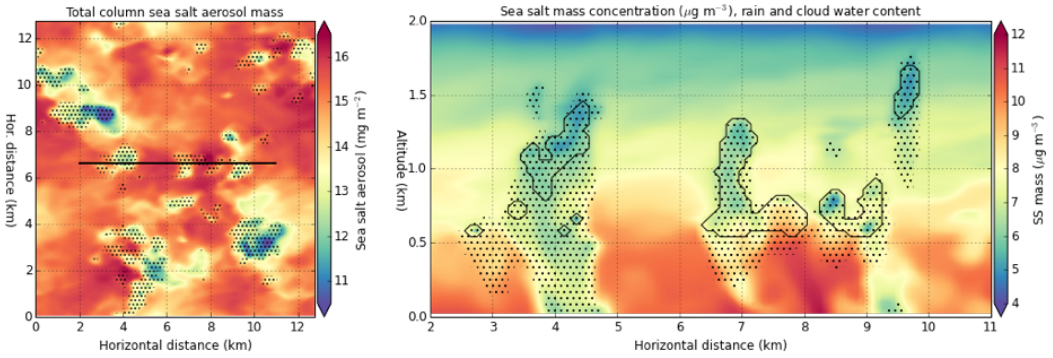

Comment 19

P11, L7: "κ-KAPPA"

Response & Changes Typo corrected to "KAPPA".

Comment 20

P13, Fig. 3 (and Fig. 4): Altitude range could be increased to show also cloud tops.

Response & Changes Cloud tops in our simulation do not reach much further than 2500 m. We left out the upper- most part of the vertical profile here because the statistics in Fig. 3 can be misleading at the highest levels because very few clouds reach that altitude. We chose the vertical range in Fig. 4 to be consistent with Fig. 3. Nevertheless, we will increase the

altitude range to include all cloud tops in both figures.

Comment 21

P17, L11-12: Unclear sentence

Response & Changes We have rewritten the sentence to immediately make clear that we compare the fate of the in-rain aerosol vs. the fate of rainwater itself:

"The abovementioned balance between the two sink processes for in-rain aerosol (i.e., resuspension vs. sedimentation) is substantially different than for the rainwater itself, in which 93 (KAPPA) or 83% (PN) of the falling precipitation evaporates leading to the resuspension of only 50-55% of the in-rain aerosol mass."

Comment 22

P19, Table 5 and related text: Maybe 1 nm accuracy would be good enough?

Response & Changes Agreed, we adopt the suggested accuracy of 1 nm.

Comment 23

P27 -: Journal names should be abbreviated

Response & Changes We checked the complete list of references and abbreviated all journal names using Caltech Library Services (www.library.caltech.edu/reference/abbreviations)

Comment 24

P28, L25: Manuscript is already published in GMD

Response & Changes Changed the reference to the final version: Kurppa et al. (2019)

Explicit aerosol-cloud ~~interaction~~ interactions in the Dutch Atmospheric Large-Eddy Simulation model DALES4.1-M7

Marco de Bruine[1,2], Maarten Krol[1,2], Jordi Vilà-Guerau de Arellano[2], and Thomas Röckmann[1]

[1]Institute for Marine and Atmospheric Research Utrecht, Utrecht University, Utrecht, The Netherlands
[2]Department of Meteorology and Air Quality, Wageningen University, Wageningen, The Netherlands

Correspondence to: M. de Bruine (m.debruine@uu.nl)

Abstract. Large-Eddy Simulations (LES) are an excellent tool to improve our understanding of the aerosol-cloud ~~interaction~~ interactions (ACI). ~~These models combine a spatial resolution high enough to resolve cloud structures with domain sizes large enough to simulate macroscale dynamics and feedback between clouds. However, most research on ACI using LES simulations is focused on changes in cloud characteristics. The feedback of ACI on the aerosol population remains relatively understudied.~~ We introduce a prognostic aerosol scheme with multiple aerosol species in the Dutch Atmospheric Large-Eddy Simulation model (DALES), especially focused on simulating the ~~feedback of ACI~~ impact of cloud microphysical processes on the aerosol population. The numerical treatment of aerosol activation is a crucial element ~~in the simulation of ACI~~for simulating both cloud and aerosol characteristics. Two methods are implemented and discussed: an explicit activation scheme based on κ-Köhler theory and a more classic approach using updraft strength. ~~Model simulations are validated against observations using~~ Sample model simulations are based on the Rain in Shallow Cumulus over the Ocean (RICO) campaign, characterised by rapidly precipitating, warm-phase shallow cumulus clouds.

We find that in this pristine ocean environment virtually all ~~aerosols enter the cloud phase through activation~~ aerosol mass in cloud droplets is the result of the activation process, while in-cloud scavenging is relatively inefficient. Despite the rapid formation of precipitation, most of the in-cloud aerosol mass is returned to the atmosphere by cloud evaporation. The strength of aerosol processing through subsequent cloud cycles is found to be particularly sensitive to the activation scheme and resulting cloud characteristics. However, the precipitation processes are considerably less sensitive. Scavenging by precipitation is the dominant source for in-rain aerosol mass. About half of the in-rain aerosol reaches the surface, while the rest is released by evaporation of falling precipitation. ~~Whether ACI increases or decreases~~ The effect of cloud microphysics on the average aerosol size depends on the balance between the evaporation of clouds and rain, and ultimate removal by precipitation. Analysis of typical aerosol size associated with the different microphysical processes shows that aerosols resuspended by cloud evaporation ~~are~~ have a radius that is only 5 to 10% larger than the originally activated aerosols. In contrast, aerosols released by evaporating precipitation are an order of magnitude larger.

1 Introduction

Aerosol-cloud ~~interaction~~ interactions (ACI) ~~remains~~ remain a major source of uncertainty for future climate predictions (e.g. Boucher et al., 2013; Fan et al., 2016). The effect of changes in the aerosol population on the cloud radiative properties (Twomey, 1977) and the formation of precipitation (Albrecht, 1989) in warm-phase shallow cumulus clouds have long been recognised. However, cloud responses in different cloud regimes have proven to be complex and the net effect on climate is not well established (Rosenfeld et al., 2014). Aerosol induced changes can be buffered by compensating cloud mechanisms, e.g. the lifetime effect might be weaker than implied by simple arguments and commonly assumed in climate models (Stevens and Feingold, 2009). In convective clouds increased aerosol concentrations might invigorate updrafts and increase precipitation formation (e.g. Koren et al., 2008; Fan et al., 2018).

Although the microphysics of the cloud processes is relatively well known, the representation in global climate models (GCMs) requires simplifications accompanied by high uncertainties (e.g. Seinfeld et al., 2016). Climate models neither resolve cloud structures nor the micro-scale processes determining the cloud properties and have to rely on parameterizations. Consequently, quantification of the influence of changes in aerosol distribution on climate remains difficult. On the other side of the modelling spectrum, process-based small-scale simulations (e.g. Roelofs, 1992) describe the microphysical processes in high detail, but ~~are missing atmospheric context to determine the effects~~ cannot model the effect of aerosol-cloud ~~interaction on the macro-scale~~interactions on the macro-scale thermodynamics and structure of a cloud. To bridge this gap, cloud resolving models play a role, in particular Large-Eddy Simulation (LES) models. For these models, present-day computational power is sufficient to resolve cloud structures in mesoscale domain sizes ($> 10 \times 10$ km^2) to simulate and connect spatial and temporal scales of aerosol-cloud ~~interaction (e.g. Bretherton, 2015; Schneider et al., 2017). The high resolution~~interactions (e.g. Bretherton, 2015; Schneider et al., 2017). Typical spatial resolution and temporal resolutions of ``Ĩ0 m and ``Ĩ s are generally considered as high resolution. However, this is still too coarse to simulate the processes on particle-level that take place on the Kolmogorov length-scales in the order of 1 mm. These processes (e.g. condensation, collision-coalescence) remain parameterized in LES. Nevertheless, the resolution and explicit calculation of turbulence allows for a certain level of internal variability resulting from inter and intra-cloud variations. While some clouds develop to considerable height and produce strong precipitation, others dissipate before forming rain and their influence on the aerosol population might be very different. Moreover, ~~clouds create local disturbances to the aerosol field which influence further ACI, underlining the~~ processing of the aerosol population by one cloud influences the microphysical processes in subsequent clouds. For example, when one cloud depletes the aerosol population by wash out, this might lead to larger clouds droplets in the subsequent cloud formed on the depleted aerosol population. The might lead to faster rain formation and an even further depletion of the aerosol population. This underlines the non-linear character of ~~this interaction~~ the interaction between aerosols and clouds and the need to simultaneously simulate the clouds and the aerosol population.

LES has become a widely-used tool in research on structure and behaviour of clouds. An important research topic is the influence of changes in aerosol concentration on the cloud characteristics. However, the emphasis remains on the cloud pro-

cesses and the numerical description of the distribution of cloud water over the cloud or rain droplets. Numerous numerical methods have been developed to describe the hydrometeor size distribution. Traditionally, there was a distinction between bulk and bin schemes. In the former, droplet size distributions are described by one or more moments (total number, mass etc.) of the hydrometeor size distribution, while other moments are diagnosed from implicitly assumed size distribution shape. In bin schemes, the shape of the size distribution is more free to evolve as the particle size distribution is divided into bins of different sizes. Recent advances complemented this choice by Lagragian particle based methods like the libcloudph++ by Arabas et al. (2015) or the similar 'superdroplet' method (Riechelmann et al., 2012; Hoffmann et al., 2019). Lebo and Seinfeld (2011) deve an extensive 2D-bin method that resolves the hydrometeor characteristics as well as the solute mass dissolved in the hydrometeors. For a detailed overview and comparison of these methods see e.g. Khain et al. (2015) ~~.~~ and Grabowski et al. (2019).

In LES modelling less attention is devoted to the other side of ACI, i.e. the feedback of cloud microphysical processes on the aerosol distribution. This is reflected in the often relatively simple representation of the aerosol population. ~~Although bulk methods~~ Nowadays, methods based on a fixed cloud droplet number or (infinite) ambient aerosol concentration are almost completely replaced by ~~numerical methods taking into account~~ methods that include the aerosol size distribution ~~, composition~~in a prognostic way. Aerosol composition, however, is often assumed to be uniform.

~~Similar to the hydrometeor size distribution, for the numerical~~ In larger scale models, more attention is focused on a description of the ~~aerosol population, two methods are commonly used: modal~~ chemical composition of the aerosol population. However, due to coarse resolution and computational limitations, methods still employ traditional modal (bulk) and bin-schemes. In a modal aerosol scheme, several fixed-shape size distributions (i.e. modes) are chosen in such a way that the sum of these distributions approximates a certain (observed) aerosol population. An example of a modal scheme is M7 (Vignati et al., 2004), which will be used in this study. In bin schemes (e.g. SALSA; Kokkola et al. (2008)), the aerosol size distribution is discretised into a number of bins according to particle size. The two methods are a good example of the trade-off between accuracy and computational cost. The modal approach requires a relatively low number of prognostic variables and is computationally efficient and is used in GCMs (e.g. EC-Earth (van Noije et al., 2014) and ECHAM-HAMMOZ (Schultz et al., 2018)). However, the shape of the aerosol size distribution in each mode is assumed to always resemble a lognormal shape. The shape of the total aerosol distribution in bin schemes is more free to evolve, but this comes at a much higher computational cost.

Recent ~~advances regarding the description of aerosols within LES models~~ examples of studies with a focus on multiple aerosol species and/or (aqueous-phase) chemistry are the inclusion of the SALSA aerosol module in UCLALES (Tonttila et al., 2017) and PALM (Kurppa et al., 2019). This bin scheme allows for multiple aerosol species, but the added value of taking into account the aerosol composition on simulating clouds in an LES model has not yet been explored. The implementation in UCLALES still uses a uniform composition in the aerosol distribution, while the study with the PALM model is focused on urban climates under dry conditions. Another promising example is the aqueous-phase chemistry extension of the libcloudph++ library (Arabas et al., 2015), described in Jaruga and Pawlowska (2018). The added attributes of chemical composition to the superdroplets in this method open up a range of possibilities to interactively calculate multiple aerosol

species and their behaviour in clouds and precipitation.

~~In this work, we take a step forward with the DALES model and combine the detailed implementation of the microphysical cloud processes with a comprehensive representation of the aerosol distribution.We~~ In this work, we focus on closing the loop of aerosol-cloud ~~interaction~~ interactions and quantify the contribution of different cloud processes to changes in the aerosol distribution. We take a step forward with the DALES model and combine microphysical cloud processes with M7 (Vignati et al., 2004): a multi-species, modal representation of the aerosol distribution. From the perspective of pollution and atmospheric budgets, we opted to implement an aerosol framework with multiple species. ~~Moreover, this~~ This also allows for explicit calculation of aerosol ~~activation~~ characteristics like hygroscopicity. Consequently, aerosol activation can based on the characteristics of the aerosol population~~.~~ , instead of using a parameterization solely based on e.g. updraft velocity. Including multiple aerosol species also allows for a better future coupling to gas-phase chemistry and semi-volatile species and accommodates emission-based simulations, so that less assumptions on the atmospheric composition are needed. In contrast to the SALSA and libcloudph++ aerosol frameworks, the computational cost of M7 is considerably lower and allows for longer simulations.

This work is motivated by our earlier work (de Bruine et al., 2018) in which the removal of aerosol by clouds on the global scale using the EC-Earth-TM5 model was investigated. This work showed that different (reasonable) choices in the parameterization of wet removal have a considerable impact on simulated global aerosol burdens. By revisiting the aerosol-cloud ~~interaction~~ interactions in LES simulations we aim to answer the following questions:

- What are the effects of the aerosol-cloud ~~interaction~~ interactions on the aerosol (size) distribution?
- How do the characteristics of the aerosol change due to cloud processes, and which cloud processes are responsible?
- Does the relative importance of the different microphysical processes change for different aerosol species (e.g. small vs. coarse or hygroscopic vs. hygrophobic aerosol)?

The paper is structured as follows. A short description of the standard version of the DALES model and cloud microphysics numerical scheme is given in Sect. 2~~. The implementation of the~~ , together with a more elaborate explanation of the new modal aerosol scheme and additional cloud-microphysical calculations ~~are presented~~ in Sect. 2.1. The case set-up and simulation ensemble are outlined in Sect. ~~3~~3.1. The results are ~~compared to and validated against observations of the~~ separated into two parts: the differences in cloud microphysical properties between simulations is discussed in Sect. 3.1.1 ~~. The feedback of ACI on aerosol characteristics is discussed~~ and the effects on the aerosol characteristics in Sect. 3.1.1. The overall results are discussed in Sect. 4 and general conclusions are drawn in Sect. 5.

2 Model description

The model used in this study is the Dutch Atmospheric Large-Eddy Simulation (DALES) (Heus et al., 2010; Ouwersloot et al., 2017), version 4.1. DALES ~~is a large-eddy simulation model~~ was initially designed to study the physics of the atmospheric

boundary layer. Previous research has expanded the application of DALES and combines the physics with chemistry and biology. Applications using the DALES model include (gas-phase) chemistry (e.g. Vilà-Guerau de Arellano et al., 2011), direct aerosol effects (Barbaro et al., 2013, 2014), semi-volatile species (Aan de Brugh et al., 2013), and interaction with the biosphere (Vilà-Guerau de Arellano et al., 2014).

In this study we conduct simulations at a horizontal resolution of $\Delta x = \Delta y = 100$ m with a domain size of 12.8×12.8 km^2 using a periodic boundary condition. The vertical resolution is $\Delta z = 40$ m with a domain height of 5040 m. The time step is limited by the Courant-Friedrichs-Lewy (CFL) criterion and diffusion number (Wesseling, 1996) but never longer than 2 s. ~~The timespan of the simulations is 6 hours.~~ Time integration is done using a third-order Runge-Kutta scheme based on the work of Wicker and Skamarock (2002). Advection is calculated using a 5th-order scheme for momentum and heat, while a monotonous scheme (Hundsdorfer et al., 1995) is used for moisture and aerosol fields to ensure positive values.

~~In the standard version of DALES~~

2.1 Dynamics and moist processes

In DALES version 4.1, the cloud-microphysical scheme is a bulk scheme for precipitating liquid-phase clouds, distinguishing between cloud water and precipitation. Cloud liquid water is diagnosed using a classic saturation adjustment (Sommeria and Deardorff, 1977). The cloud droplet number concentration is a fixed parameter, regardless of simulated amount of cloud water. However, the cloud droplet number concentration can be adjusted to simulate different pollution levels.

For the calculation of precipitation, two schemes have been implemented in DALES. The first scheme is based on Seifert and Beheng (2001), with updated numerical representation of the rain drop size distribution and sedimentation (Seifert and Beheng, 2006; Stevens and Seifert, 2008), and rain evaporation (Seifert, 2008). In the remainder of this work, this scheme is referred to as the SB scheme. The second cloud scheme is based on Khairoutdinov and Kogan (2000), but is valid only for (drizzle formation in) stratocumulus clouds. In this work, we will simulate shallow cumulus and thus use the SB scheme. For more information and details on the implementation of this scheme in DALES, see Section 2.8 of Heus et al. (2010).

3 ~~Aerosol framework~~

2.1 Aerosol framework

The aerosol population is described by the modal aerosol scheme M7 (Vignati et al., 2004). ~~This framework allows for the simulation of an external mixture of aerosol species, so that the differences in feedback of ACI on the different aerosol species can be investigated. Also, by~~ The modal representation is compatible to the existing SB cloud microphysics scheme since this uses a 2-moment bulk approach as well. By using M7, cloud activation can be based on fundamental principles linked to the explicit simulation of the properties of the aerosol species (see Sect. 2.1.1). Moreover, ~~the modal representation of the aerosols~~

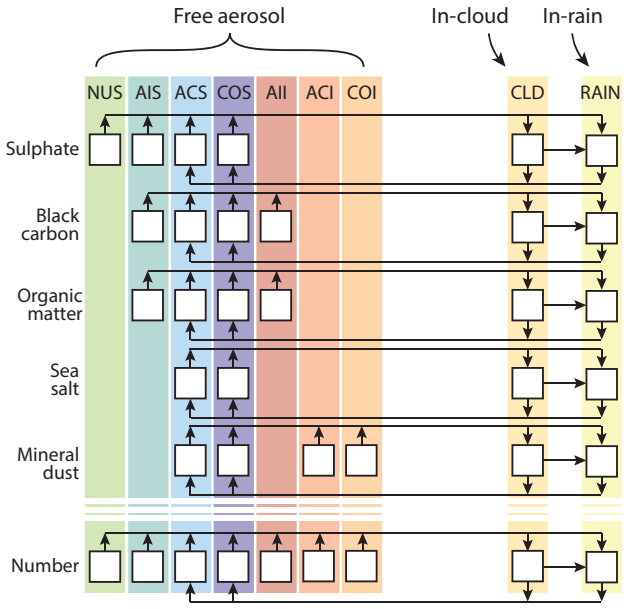

Figure 1. Overview of the aerosol framework, where the free aerosol section is the original M7 representation of the aerosol population. The extension of this framework in the current work is represented by the prognostic variables for in-cloud and in-rain aerosol mass. Cloud and rain particle number coincide with the corresponding parameters in the SB bulk microphysics scheme. Arrows represent possible pathways for the aerosols to transfer between states.

~~is compatible to the existing SB cloud microphysics scheme since this uses a 2-moment bulk approach as well. Calculations of the cloud~~ calculations of the cloud microphysical processes can ~~thus~~ also be directly linked to their influence on the aerosol distribution. This framework allows for the simulation of an external mixture of multiple aerosol species. In future development, this will be coupled to atmospheric chemistry, including aqueous-phase chemistry.

2.1.1 Numerical representation

In the M7 scheme (see Fig. 1) the aerosol population is described by a combination of 5 aerosol species: sulphate, black carbon, particulate organic matter, sea salt and mineral dust. The aerosol species are distributed over 7 lognormal modes~~with a prescribed width~~, hence the name M7, with prescribed mode widths σ. Four of these modes represent soluble aerosols of different sizes, i.e. nucleation, Aitken, accumulation and coarse size and are abbreviated as: NUS, AIS, ACS, and COS. The remaining 3 modes represent insoluble aerosol in the sizes of Aitken, accumulation and coarse aerosol, abbreviated as AII, ACI and COI. As visualised in Fig. 1, each mode is described by 1 prognostic variable for number concentration, plus a maximum of 5 variables for the mass of the different aerosol species that are contained in that mode. For example, the Aitken soluble mode contains the masses of 3 species (sulphate, black carbon and organic matter) and thus has $1 + 3 = 4$ prognostic variables. The M7 framework includes a numerical treatment for temporal evolution, or 'ageing', by e.g. coagulation as well as sedimentation

of the aerosol. However, these are not applied in this work as the associated timescales for these processes are long compared to those of the interaction between aerosol, clouds and precipitation.

To connect the description of aerosol to the SB microphysics scheme, the M7 framework is extended with two additional modes containing the in-hydrometeor (i.e. cloud droplet ~~or~~ and raindrop) aerosol. Similar to the free aerosol modes, both the in-cloud and in-rain aerosols are described by 1 variable for number concentration and 5 for the in-hydrometeor aerosol mass concentration for each aerosol species. ~~An important implication of this approach is that size (and mass) information of the originating free aerosol mode is lost once aerosols are incorporated in cloud and raindrops. Another consequence is~~ This modal approach leads to the implicit assumption that the in-hydrometeor aerosol mass is homogeneously distributed ~~across~~ over the cloud or rain drop distributions, i.e. aerosol concentrations do not change with hydrometeor size. As a result, size (and mass) information of the original free aerosol mode is lost once aerosols are incorporated in cloud and raindrops. In more technical terms: the external mixture of 7 modes for the free aerosol is transformed to one internal mixture of aerosols in the hydrometeor mode. Although this approach might not be completely realistic, the aerosol distribution in clouds and rain have been found to be homogeneous in later stages of the cloud lifecycle due to frequent collision-coalescence (e.g. Roelofs, 1992).

Note that the cloud and rain droplet modes do not necessarily need to have a lognormal shape like the aerosol modes. Instead, ~~they are described by a~~ the SB microphysics scheme assumes generalised Γ-distribution, better resembling the droplet size distributions found in clouds and rain. The cloud droplet number N_c and raindrop number N_r are used in the calculations of the ~~SB microphysicsscheme~~cloud microphysics, together with cloud liquid water q_c and rain water q_r.

2.2 ~~Microphysical processes~~

The combination of the aerosol framework and the individual microphysical processes opens up the opportunity to explicitly simulate the transfer of aerosol between the free, in-cloud and in-rain aerosol state by the individual processes. The ~~numerical implementation of~~ current numerical implementation focuses on the mode-specific activation ~~as well as~~ and size resolved aerosol scavenging ~~are~~ described in this section. Note that there are numerous other processes involved in the interaction between aerosols and clouds. Our framework is not yet linked to the calculation of (gas-phase) chemistry. Also, our model does not include aqueous-phase oxidation of dissolved species which might influence the aerosol size distribution (e.g., Feingold and Kreidenweis, 2002; Ovchinnikov and Easter, 2010)). Neither does our model calculate the formation of secondary aerosol nor the influence clouds can have on that process (e.g., Wehner et al., 2015).

2.1.1 Activation

In the new aerosol representation, activation of aerosols can be based on the κ-Köhler method as defined in Petters and Kreidenweis (2007). This method describes the relationship between the dry radius of a particle and its ability to act as cloud condensation nucleus (CCN), where hygroscopicity is expressed in a single hygroscopicity parameter κ. At a given supersaturation S and depending on hygroscopicity, aerosols with a radius larger than the critical radius r_c will be activated to form

cloud droplets. Based on Eq. (10) in Petters and Kreidenweis (2007), r_c is calculated for the aerosol mode k as:

$$r_{c,k} = \left(\frac{4\,A^3}{27\,\kappa_k\,\ln^2 S} \right)^{1/3}, \text{with } A = \frac{4\sigma_{s/a} M_w}{R\,T\,\rho_w} \tag{1}$$

with mode mean hygroscopic parameter κ_k (unitless), supersaturation (saturation ratio) S (unitless), surface tension of a water-air interface $\sigma_{s/a}$ (J m^{-2}), molar mass of water M_w (kg mol^{-1}), density of water ρ_w (kg m^{-3}), gas constant R (J mol^{-1} K^{-1}) and ambient temperature T (K). Note that $r_{c,k}$ (m) can change between aerosol modes as κ_k depends on the relative mass of the aerosol species within a mode~~.~~, calculated following Eq. (5).

Using the lognormal properties of the M7 aerosol modes, the activated fraction of aerosol for mode k is given by:

$$f_k = 1 - \frac{1}{2}\,\mathrm{erfc}\left(-\frac{\ln(r_{c,k}/\widetilde{r}_k)}{\sqrt{2}\ln(\sigma_k)} \right) \tag{2}$$

where $\widetilde{r}_k$ is the mode median radius and σ_k is the mode geometric standard deviation. This equation can be applied to both aerosol number and aerosol mass by replacing $\widetilde{r}_k$ by the number median radius $r_{n,k}$ or mass median radius $r_{m,k}$ respectively. These are calculated as:

$$r_{n,k} = \left(\frac{6M_k}{\pi N_k \rho_k} \right)^{1/3} \exp\left(-\frac{3\ln^2 \sigma_k}{2} \right) \tag{3}$$

$$r_{m,k} = r_{n,k} \exp(3\ln^2(\sigma_k)) \tag{4}$$

with N_k (kg^{-1}) the aerosol number concentration, M_k (kg kg^{-1}) the sum of the aerosol mass concentrations of all species and ρ_k (kg m^{-3}) the mean aerosol density in mode k.

Mean properties for each mode k are calculated as the volume-mean averages of the different aerosol species i within that mode, following:

$$\varphi_k = \frac{\sum_i m_{i,k}}{\sum_i m_{i,k}/\varphi_i} \frac{\sum_i V_{i,k}\varphi_i}{\sum_i V_{i,k}}, \quad V_{i,k} = \frac{m_{i,k}}{\rho_i} \tag{5}$$

Here, $V_{i,k}$ and $m_{i,k}$ is the volume and mass of species i in mode k. φ_i is substituted by the species-specific hygroscopic parameter κ or density ρ (kg m^{-3}) to calculate the mode mean values used in Eq. (1) and (3). Values for density ρ and the hygroscopic parameter κ for the five M7 aerosol species are given in Table 1.

As stated above, DALES uses an '~~-~~'all-or-nothing' ~~cloud water adjustment~~ saturation adjustment scheme in which cloud liquid water q_c is a diagnostic variable. Therefore, we use a fixed value of supersaturation (~~$S = 0.4\%$)~~ $S = 0.4\%$) in Eq. (1) which is representative for the simulated case (Derksen et al., 2009). ~~Although fixing the~~ However, by fixing S, the model omits the competition for moisture between particles (aerosols and cloud droplets) or the role of supersaturation in this process.

Table 1. Values of density ρ and the hygroscopic parameter κ for the five aerosol species considered in M7.

	ρ (kg m^{-3})*	κ (-)**
Sulphate	1841	0.88
Black carbon	1300	0
Organic matter	1800	0.1
Sea salt	2165	1.28
Mineral dust	2650	0

*van Noije et al. (2014), **Pringle et al. (2010)

Moreover, by directly linking supersaturation levels to particle activation, we implicitly assume that the equilibration time of the droplets is instantaneous or considerably shorter than the model timestep. This might lead to an overestimation of activated droplets as some particles would activate at a certain supersaturation, but did not have enough time to grow to the respective critical radius. This process would be better captured by a numerical framework that directly calculates condensational growth. However, including this in a multi-species aerosol scheme would be computationally too demanding. To asses the impact of using a fixed supersaturation on the cloud characteristics in our simulations, we will perform sensitivity simulations with different values of S. Although fixing the value of S is ~~still an approximation which can be further investigated in the future, the new framework is a substantial improvement as it allows~~ an approximation, it does allow for an interactive calculation of cloud droplet number concentration based on simulated aerosol. ~~Additionally, we will perform a series of sensitivity simulations to assess the impact of changing supersaturation values on the cloud characteristics.~~

~~Values of density ρ and the hygroscopic parameter κ for the five aerosol species considered in M7. ρ (kg m^{-3})*~~ A modal representation of the aerosol size distribution poses a fundamental problem for the numerical calculation of aerosol activation. Cloud activation strongly modifies the shape of the aerosol size distribution by removing the larger particles exclusively. However, in the subsequent timestep, the model again assumes a full lognormal distribution. This effectively redistributes aerosol mass and number to all sizes of the lognormal size distribution, including aerosols exceeding the critical radius which allows for additional activation. Frequent repeated activation and re-distribution of aerosol might lead to a possible 'runaway activation' which depletes the complete aerosol population and yields unrealistically high cloud droplet number. To avoid this 'runaway activation' in the κ~~(-)**~~ Köhlker-based scheme, activation in a cloudy grid cell is allowed only once. Additional activation is suppressed until the grid cell becomes cloud-free again.

~~Sulphate 1841 0.88 Black carbon 1300 0 Organic matter 1800 0.1 Sea salt 2165 1.28 Mineral dust 2650 0~~

To be able to disentangle effects of the numerical description of activation from other processes, an alternative method for activation is implemented. This method is based on the work of Pousse-Nottelmann et al. (2015), hereinafter PN15. This

activation method is also geared towards a modal representation of the aerosol distribution, but calculates N_c using updraft velocity w and the number concentration of soluble mode particles larger than 35 nm $N_{>35}$ ~~.~~as given by Eq. (2) in PN15:

$$\left.\frac{\partial N_c}{\partial t}\right|_{\text{acti}} = \max\left\{\frac{1}{\Delta t}\left[0.1\left(\frac{wN^t_{>35}}{w+\alpha N^t_{>35}}\right)^{1.27} - N_c^{t-1}\right], 0\right\}, \tag{6}$$

with w the updraft vertical velocity, Δt the length of the timestep, N_c^{t-1} the number of cloud droplets present, $N^t_{>35}$ the number concentration of soluble/mixed aerosol particles larger than 35 nm and $\alpha = 0.023$ cm^4 s^{-1} an empirically derived constant. $N_{>35}$ is calculated as the sum of the soluble accumulation and coarse mode number concentrations, plus the fraction of soluble Aitken mode particles above 35 nm, evaluated using Eq. (2). As described in PN15, activation is assumed to progress from the biggest to the smallest particles in each mode.

~~A modal representation of the aerosol size distribution poses a fundamental problem for the numerical calculation of aerosol activation . Cloud activation strongly modifies the shape of the aerosol size distribution by removing the larger particlesexclusively~~

By including updraft velocity w and the existing cloud droplet number N_c^{t-1}, this formulation does include competition for moisture between condensation on existing droplets and activation of new particles. However, ~~in the subsequent timestep, the model again assumes a full lognormal distribution. This effectively redistributes the aerosol to all sizes of the lognormal size distribution, including aerosols exceeding the critical radiuswhich allows for additional activation. To avoid this '~~the strongest limitation of this formulation is found in the prefactor of 0.1. This prefactor was determined in Zubler et al. (2011a) by comparison of their model outcome against satellite data with respect to the cloud droplet effective radius. The combination of this prefactor and the subtraction of N_c^{t-1} poses such a strong limitation on aerosol activation that 'runaway activation' ~~, in the KAPPA scheme activation in a cloudy grid cell is allowed only once. Additional activation is suppressed until the grid cell becomes cloud-free again. In the PN activation scheme, this effect is negated by setting the lower limit for activation to 35 nm, and subtracting N_c from the calculated amount of activated aerosols~~does not occur in the PN scheme.

2.1.2 Scavenging

With the addition of prognostic variables for the aerosol population, scavenging has to be addressed in the aerosol budget. Our implementation of aerosol scavenging is based on the framework of Croft et al. (2009, 2010) and distinguishes between scavenging by cloud droplets (i.e. in-cloud scavenging) and by falling precipitation (i.e. below-cloud scavenging). Because scavenging by falling raindrops also takes place within a cloud, this process is referred to as rain scavenging in the remainder of this work to avoid confusion. The separation of scavenging by cloud droplets and precipitation matches the description in the cloud microphysics scheme that makes a similar distinction between cloud and rain droplets. ~~Similar to the original work of Croft et al. (2009, 2010),~~ The calculation of the scavenging efficiency is implemented into the model ~~as~~ using a look-up table approach. For each aerosol mode, the size-dependent scavenging efficiencies for in-cloud scavenging are determined using aerosol median radii ranging from 10^{-2} to 10^3 µm and median cloud drop radii between 5 and 50 µm. Rain scavenging is defined for aerosol median radii from 10^{-3} to 10^3 µm and rainfall intensities between 10^{-2} to 10^2 mm hr^{-1}.

2.1.3 In-hydrometeor processes

All microphysical processes that were previously implemented in DALES (i.e. autoconversion, accretion, sedimentation, self-collection and break-up) now have to take into account the in-hydrometeor aerosol mass and the transfer of aerosol mass between free, in-cloud and in-rain states. For these processes it is assumed that the aerosol mass is dissolved in the hydrometeor water and homogeneously distributed over the cloud and rain drop distributions, i.e. the aerosol concentration does not change with hydrometeor size. With this assumption, the fraction of transformed in-hydrometeor aerosol mass is equal to the transformed fraction of water. For example, if 2% of the cloud water is transformed to rain by autoconversion, 2% of the in-cloud aerosol mass is transferred to the in-rain mode as well.

With the introduction of a prognostic variable for N_c in DALES, the process of cloud droplet self-collection has to be added to the microphysical framework. For this, we use the parameterization of SB described in Seifert and Beheng (2006) Eq. (9):

$$\left.\frac{\partial N_c}{\partial t}\right|_{scsc} = -k_{cc}\frac{(\nu_c+2)}{(\nu_c+1)}\frac{\rho_0}{\rho}q_c^2 - \left.\frac{\partial N_c}{\partial t}\right|_{auau}, \tag{7}$$

where $k_{cc} = 4.44 \times 10^9$ m^{3}kg^{-2}s^{-1} is a constant describing the cloud-cloud collision efficiency, ν_c $(-)$ the width parameter in the generalised Γ-distribution for cloud droplets, ρ (kg m^{-3}) the air density, $\rho_0 = 1.225$ kg m^{-3} the reference air density and q_c cloud liquid water (kg kg^{-1}). The ~~final~~ last term on the right-hand side represents subtraction of the colliding particles involved in the autoconversion process.

2.1.4 Evaporation and aerosol resuspension

An explicit calculation of raindrop evaporation is given by the SB microphysical framework and was previously implemented in the DALES model. With the saturation adjustment approach in DALES, aerosol resuspension resulting from cloud evaporation is based on the diagnostic variable for cloud liquid water q_c and is calculated as follows. By comparing q_c of the current timestep with the value of the previous timestep, it is possible to ~~calculate~~ determine the evaporated fraction of cloud water. The corresponding transfer of aerosol particle number is calculated as:

$$\left.\frac{\partial N_c}{\partial t}\right|_{evpcevpc} = \begin{cases} \frac{q_{c,t-1}-q_{c,t}}{q_{c,t-1}}\frac{N_c}{\Delta t}, & \text{if } q_{c,t-1} > q_{c,t}. \\ 0, & \text{otherwise.} \end{cases} \tag{8}$$

By applying this relation, we implicitly assume a Marshall-Palmer size distribution for the cloud droplets, so that the evaporated fraction of cloud water equals the fraction of cloud drop number that is resuspended (de Bruine et al., 2018, Appendix A).

For the in-hydrometeor processes a one-to-one relation is used for the fraction of transferred water and the fraction associated aerosol mass. However, for the evaporation of clouds and/or rain we have to take into account that the evaporation of water does not immediately lead to the resuspension of aerosol ~~(Gong et al., 2006)~~(e.g. Gong et al., 2006). Only upon complete evaporation of a hydrometeor, aerosol mass is released. Hence, the resuspended aerosol mass fraction is not equal to the

evaporated fraction of water. We use a similar approach as de Bruine et al. (2018) to account for this effect (~~their~~ Eq. 4 therein). Additionally, as the number of aerosol particles incorporated in the hydrometeors is not explicitly tracked we apply the commonly used assumption that one evaporated hydrometeor releases one aerosol particle (Mitra et al., 1992). The resuspended aerosols are assumed to follow a lognormal size distribution with a width of $\sigma = 1.5$ (Pousse-Nottelmann et al., 2015) and are divided between the ACS and COS modes based on the aerosol radius that divides these two modes in M7, i.e. 0.5 µm (Vignati et al., 2004). The aerosols with radius < 0.5 µm are transferred to the ACS mode and the aerosols with radius > 0.5 µm are transferred to the COS mode.

~~Overview and description of the different simulations performed in this study. Name Description BASE No explicit aerosol, fixed N_c (70 cm^{-3}). BASE30 No explicit aerosol, fixed N_c (30 cm^{-3}). KAPPA Explicit aerosol, activation based on Petters and Kreidenwei $S = 0.4\%$ PN Explicit aerosol, activation based on Pousse-Nottelmann et al. (2015)SAT0.2 Similar to KAPPA except $S = 0.2\%$ SAT1.0 Similar to KAPPA except $S = 1.0\%$~~

3 ~~Case and simulation setup~~Sample simulations

3.1 Model setup

3.1.1 RICO case

To test and validate the explicit aerosol-cloud interaction framework, the simulations are based on the The Rain in Cumulus over the Ocean (RICO) field campaign (Rauber et al., 2007). This campaign, which took place during the period of November 2004 to January 2005, is characterised by shallow, precipitating maritime cumulus clouds. RICO is widely used in research on cloud processes in (trade wind) cumulus clouds, and served as the test case in an intercomparison project of twelve LES models (vanZanten et al., 2011). It is especially well-suited for the testing of our new framework because of the rapid development of precipitation, and thus including the 'full suite' of aerosol-cloud ~~interaction~~interactions. Initial profiles for moisture, temperature and wind as well as large scale tendencies and surface fluxes are the same as the those prescribed in vanZanten et al. (2011).

3.1.2 Aerosol initialisation

Although the RICO campaign did include aerosol observations, these are fairly restricted. The aerosol size distribution was measured on ~~a number of the aircraft flights, but~~ aircraft flight RF12, and the measurements were fitted to a bimodal lognormal distribution of aerosols with uniform composition, assuming characteristics of ammonium-bisulfate ~~,~~ (see vanZanten et al. (2011), Sect 2.2.3 therein), despite the marine nature of the environment. The campaign did not collect in-situ data of aerosol composition that can be used to initialise and validate the M7 aerosol variables for our simulations. Instead we use vertical aerosol profiles of the region where RICO took place from a simulation with the chemistry transport model TM5 (van Noije et al. (2014), Bergman et al. (2019)). ~~An overview is shown in Figure 2.Because this model data did not include the RICO campaign period,~~

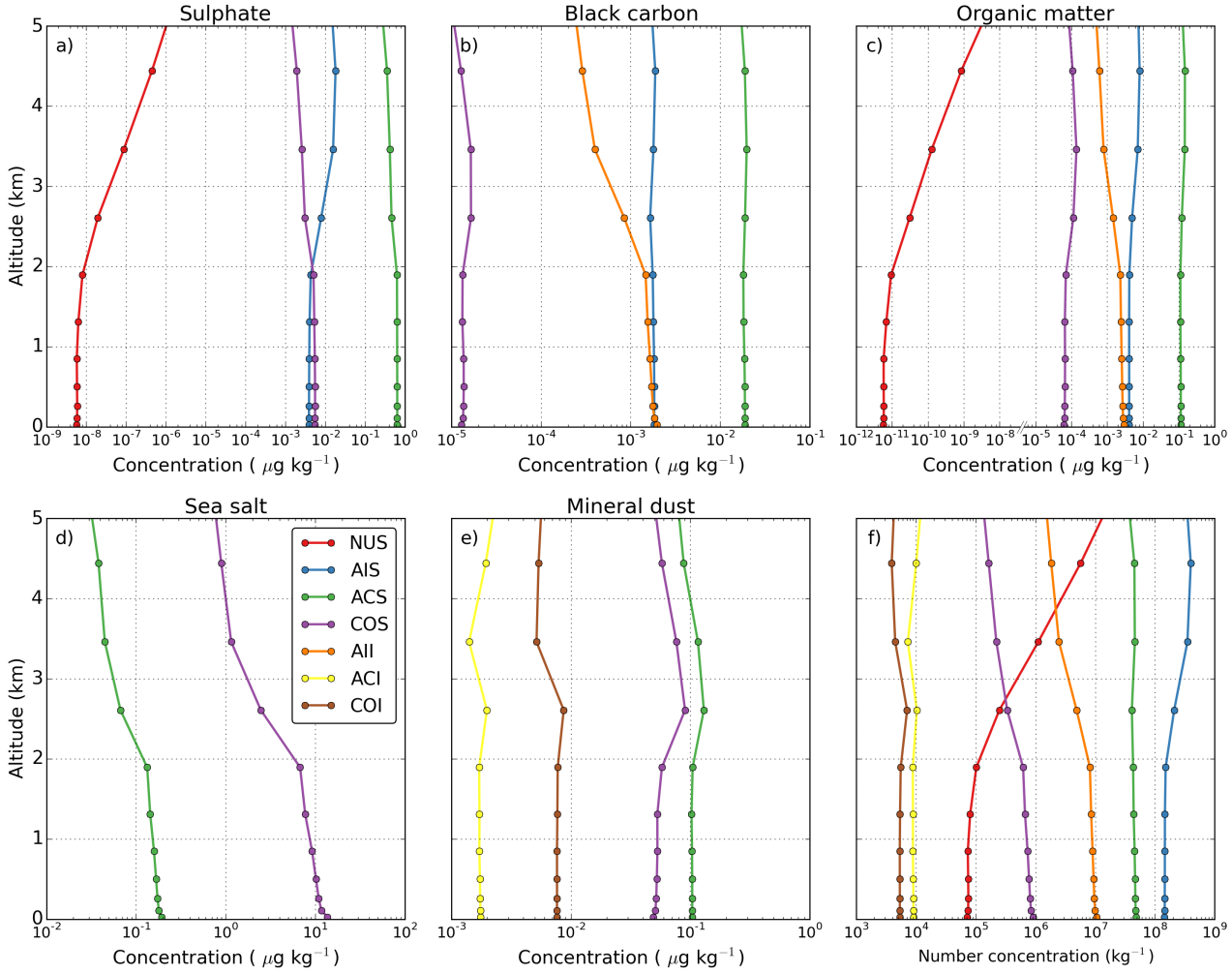

Figure 2. Initial vertical profiles of aerosol mass concentration (μg kg^{-1}) of (a) sulphate, (b) black carbon, (c) particulate organic matter, (d) sea salt, (e) mineral dust and (f) number concentration (kg^{-1}) extracted from the TM5 model (Bergman et al., 2019). Aerosol modes are specified by different colors which are consistent between panels. Circles correspond to the TM5 model levels. Note the break in the horizontal axis in panel (c).

~~an average is constructed using profiles of December 1st for the years 2006, 2008 and 2010.~~ The simulations were originally carried out for a remote sensing experiment within the Aerocom project (http://aerocom.met.no) by the Dutch Meteorological Institute (KNMI) in 2017.

~~As expected for a region~~ Since TM5 uses the same modal aerosol framework M7, a one-to-one translation of the aerosol scalar fields can be made. The only difference between the latest version of TM5 (Bergman et al., 2019) and DALES in the aerosol representation is the inclusion of secondary organic aerosol in the TM5 model. This is expressed in the presence of

POM in the soluble nucleation (NUS) mode which does not exist in DALES. The corresponding mass is negligible, but is incorporated in the POM Aitken soluble (AIS) mode mass nevertheless.

The TM5 output is provided on native model pressure fields. These pressure fields are transformed to altitude coordinates using corresponding temperature fields. Since our simulations concern a case over the ocean, ~~the~~ no corrections for topography are needed. The resulting transformation yields 9 levels in the lowest 5000 m, which is the vertical extent of the DALES model simulations. Of these pressure levels, 4 are located near the surface (i.e. below 1000 m). Linear interpolation is used between these levels and the values between top and bottom of DALES gridboxes are averaged and assigned to the DALES vertical grid. Resulting profiles are shown in Fig. 2.

The aerosol population mainly consists of sea salt particles~~. The average~~ , as expected for this ocean region with trade winds blowing from the open ocean. The sea salt mass concentration in the lowest 2000 m is 10.0 µg m^{-3}~~, accounting for 90% of the total aerosol mass. Due to the fact that sea salt is a locally generated species, mass concentration decreases with height. The~~ . The other species account for 0.69 µg m^{-3} (sulphate), 0.19 µg m^{-3} (mineral dust), 0.14 µg m^{-3} (organic matter) and 0.027 µg m^{-3} (black carbon). Additionally, the sea salt mass concentration shows a decrease with height, explained by the fact that it is locally generated. The concentrations of the other species are more or less constant with height ~~, typical for non-local species~~ or even show a slight increase with height. For the pristine environment in the RICO campaign, these species are advected into the region ~~. The average aerosol~~ and display characteristics of an aged aerosol population. For example, the mineral dust particles are considerably smaller than the sea salt particles and mainly reside in the soluble modes.

The total number concentration in the lowest 2000 m is 202 cm^{-3}, ~~of which 82.6~~ mainly consisting of Aitken mode particles (149.6 cm^{-3}~~activates~~). Of all aerosol particles, 82.59 cm^{-3} activate at a supersaturation of 0.4%. This ~~theoretical value is calculated using~~ value is diagnosed by applying the κ-Köhler ~~method with the hygroscopicity values described~~ theory with the characteristic values of the different species shown in Table 1. ~~A more detailed description of the aerosolinitial conditions is given in Appendix A~~

3.1.3 Overview

To establish a baseline for the model results, the first simulation (BASE) uses the base version of DALES. This version uses a prescribed, fixed cloud drop number concentration (i.e. 70 cm^{-3}) and follows the settings described for the model intercomparison of vanZanten et al. (2011). The second simulation uses a lower cloud drop number concentration (30 cm^{-3}) which corresponds to the actual observed mean values (see Sect 3.1.1). This simulation is referred to as BASE30. ~~In the κ-KAPPA~~

In the KAPPA simulation, aerosols are activated using the κ-Köhler-based aerosol activation scheme. Based on this simulation, two sensitivity simulations are performed using supersaturations of 0.2% and 1.0% (SAT0.2 and SAT1.0 respectively). To test the results of the κ-Köhler activation, the alternative activation scheme of Pousse-Nottelmann et al. (2015) is used in the PN simulation. An overview of the different simulations is given in Table 2. ~~The total length of the simulations is~~ Because we do not simulate the emission of new aerosol during the simulations, the originally 24 hour-long simulations in vanZanten et al. (2011) are shortened to 6 hours~~, of which the last~~ . In longer simulations, the wash-out by precipitation would

Table 2. Overview and description of the different simulations performed in this study.

Name	Description
BASE	No explicit aerosol, fixed N_c (70 cm^{-3}).
BASE30	No explicit aerosol, fixed N_c (30 cm^{-3}).
KAPPA	Explicit aerosol, activation based on Petters and Kreidenweis (2007) with $S = 0.4\%$
PN	Explicit aerosol, activation based on Pousse-Nottelmann et al. (2015)
SAT0.2	Similar to KAPPA except $S = 0.2\%$
SAT1.0	Similar to KAPPA except $S = 1.0\%$

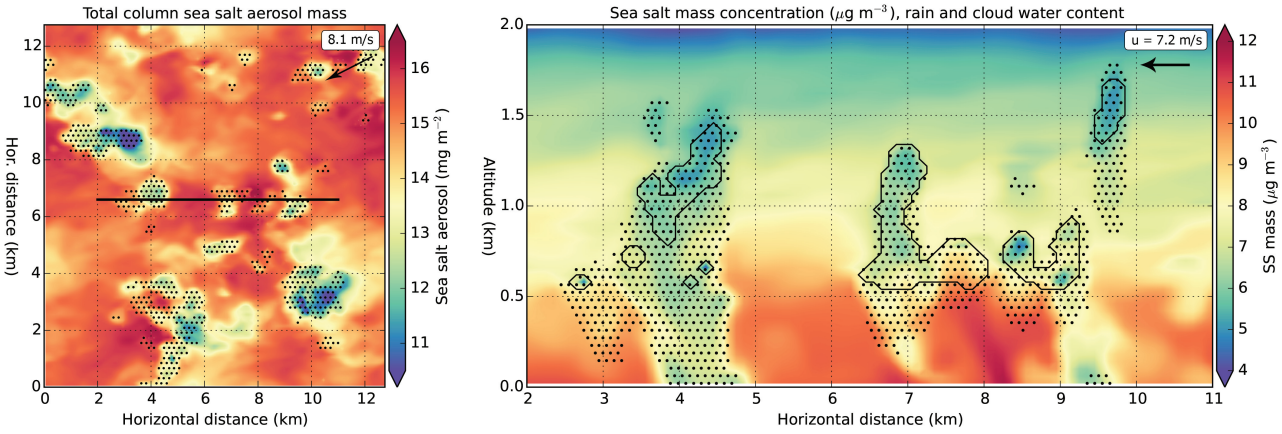

Figure 3. ~~Instantaneous horizontal~~ (left) ~~and vertical (right)~~ Instantaneous horizontal cross sections of the cloud and aerosol spatial distribution at $t = 5.5$ hours. Occurrence of clouds and precipitation is indicated by the hatched areas. The underlying color scale indicates sea salt aerosol mass concentration. Average wind speed and direction in the cloud layer (500 - 2000 m) is denoted in the top-right corner~~of the left panel~~. The ~~zonal component of~~ black line indicates the ~~wind is~~ vertical cross-section shown in the right panel. ~~The location of the~~ (right) Vertical cross-section ~~shown~~ of sea salt aerosol concentration, with cloud (outline) and precipitation (hatching) indicated separately. Arrow in the top right ~~panel is indicated by~~ corner indicates the ~~black line in~~ zonal component of the ~~top-down overview~~wind.

deplete the aerosol population to unrealistically low levels. The first 3 hours ~~are used~~ of the simulation are considered spin-up and discarded in the analysis ~~.~~ of the results. Although the simulation has not yet fully equilibrated after 3 hours, metrics like liquid water path and cloud fraction only show a slow change after that as can be seen in e.g. Fig 3 in vanZanten et al. (2011).

4 ~~Results~~

3.1 Results

A qualitative overview of the simulated cloud scene for the RICO campaign is shown in Fig. 3. These cross-sections ~~beautifully display the richness of LES simulations with the internal variability~~ display the internal variability within the LES model domain that results from ~~resolving most of the turbulence~~the high spatial resolution. Both large and small cloud structures are found in the simulated domain, and developing clouds coexist with readily precipitating clouds. Simulations show characteristics typical for shallow cumulus clouds, which is in accordance with observations. Clouds are sparsely spread over the domain, covering about 10% of the total sky. The cloud base is located at about 500 m and cloud tops reach up to 2000-2500 m.

The interaction between the clouds and aerosol is clearly visible in the strong reduction of aerosol mass in the presence of liquid water. In addition, changes to the aerosol distribution as a result of ~~ACI~~ cloud processing and/or wash-out are reflected in the inhomogeneities of the aerosol field in the regions where clouds no longer exist. More details of ~~ACI~~ the influence of clouds and precipitation on the aerosol concenration are shown in the right-hand panel of Fig. 3. Here, we can observe a decreased aerosol concentration in the ~~wake located right of the~~ precipitation field (around ~~6km)as the general flow moves the clouds from right to left in this figure~~4 km). In contrast, an increased aerosol concentration is found ~~at left side of the same cloud~~ below the clouds (around 8 km) as a result of evaporating precipitation between cloud base and the surface.

Further results of the simulations will be discussed in two steps. Section 3.1.1 will focus on the cloud characteristics and compare ~~modelled values to observations~~the results of the different simulations. Section 3.1.1 addresses the ~~other side of ACI: the feedback~~ effect of the cloud microphysics on the aerosol distribution. The strength of the aerosol fluxes associated with the cloud microphysical processes are quantified as well as the location in the vertical column where these processes take place. In addition, the differences between the aerosol species are discussed. Particular attention is given to the typical aerosol size associated with the various processes in clouds and precipitation.

3.2 ~~Cloud microphysics~~

3.1.1 Cloud microphysics

To ~~validate~~ evaluate the modelled cloud characteristics produced in the different simulations we follow the ~~the~~ analysis of vanZanten et al. (2011). ~~Measurements are taken from 6 aircraft flights performed during the RICO campaign.~~ Domain-averaged cloud characteristics are shown in Fig. 4, which is constructed to resemble Fig. 8 in vanZanten et al. (2011). Similar to their work ~~, simulated cloud~~ we use an aggregate of 1 Hz FFSSP measurements on flights RF06-RF12 with the C-130 aircraft (Rauber et al., 2007). Cloud characteristics are filtered using the condition $q_c > 0.01$ g kg^{-1}, while rain characteristics use the condition $q_r > 0.001$ g kg^{-1}.

The ~~RICO campaign in-situ~~ above-mentioned aircraft observations show values for N_c up to 90 cm^{-3}, but mean values are around 30 cm^{-3}, while median values are about 20 cm^{-3}, slightly decreasing with altitude. This is considerably lower than

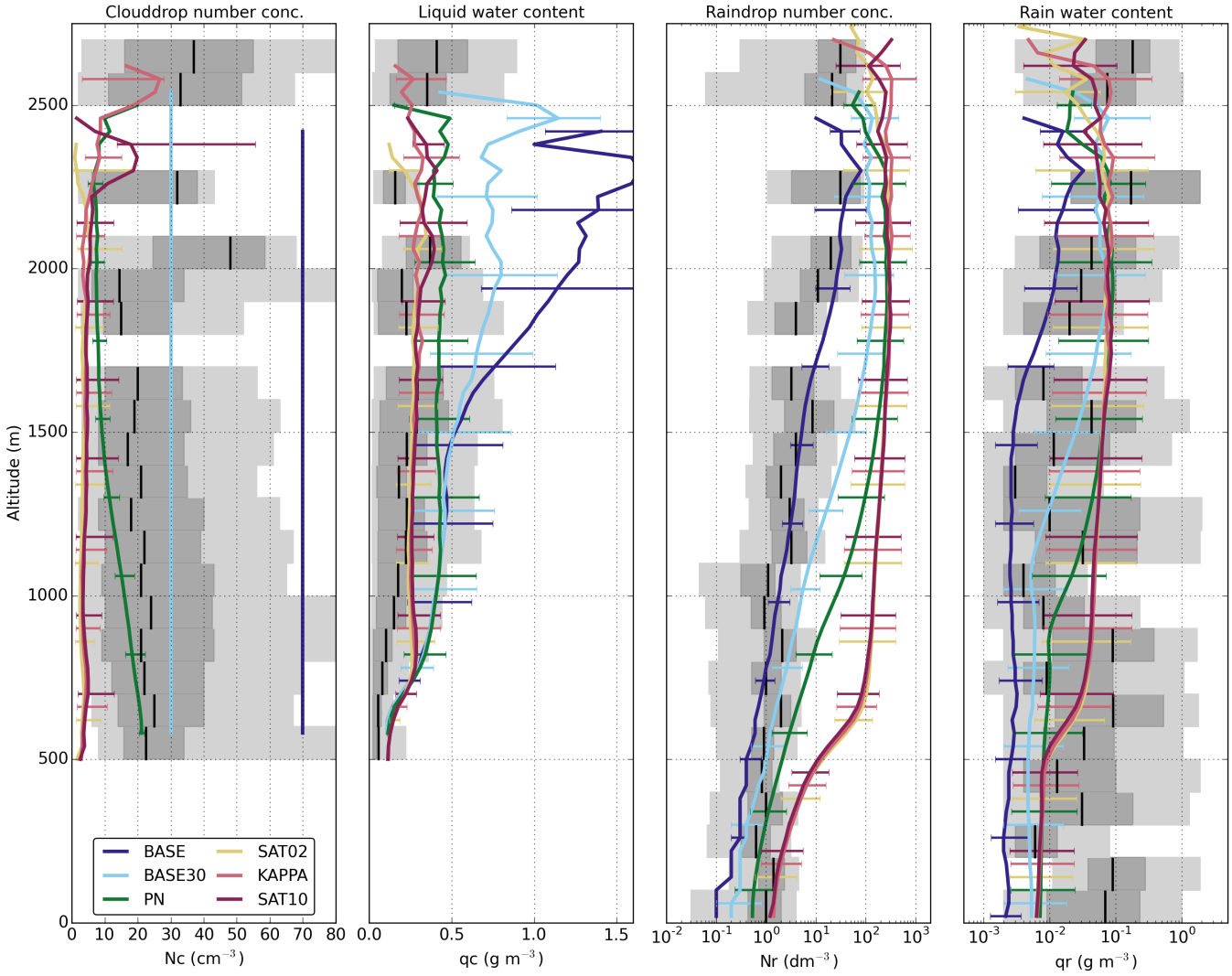

Figure 4. Validation of modeled cloud and rain characteristics against observations of a) cloud droplet number concentration N_c, b) cloud liquid water q_c, c) rain drop number concentration N_r and d) rain water content q_r. Observations are grouped by altitude using increments of 100 m. Median value is shown by vertical black bars, light grey shading indicates the 5th to 95th percentile, while dark grey indicates 25th to 75th percentile. Median simulated values are represented by colored lines with the errorbars indicating the 25th to 75th percentile.

the default fixed value of N_c of 70 cm^{-3} ~~for this case~~ used in the BASE simulation, which was the prescribed value for the simulations in vanZanten et al. (2011). The BASE30 simulation uses $N_c = 30$ cm^{-3}, ~~which resembles the observed~~ based on the observed mean N_c ~~values better~~of the aircraft observations. In the other simulations, N_c is not prescribed but interactively calculated from the aerosol distribution. The new framework with explicit κ-Köhler activation used in the KAPPA simulation ~~underestimates~~ yields values for N_c ~~with values~~ of about 4-10 cm^{-3}~~, without a distinct change with height~~. Increasing the

values for critical supersaturation to 1% in the SAT1.0 simulation ~~does not show a significant increase in~~ shows an insignificant increase in median N_c ~~, nor does a decrease~~ of about 1 cm^{-3}. Decreasing S to 0.2% in the SAT0.2 simulation shows a similar decrease the modelled amount of N_c. When using the alternative activation scheme in the PN simulation, N_c values of 30 cm^{-3} are found at cloud base, but N_c decreases to about 10 cm^{-3} at an altitude of about 1500 m and remains constant above this level.

~~For the cloud water liquid content q_c, the observations show a continuous increase with height (as expected for shallow cumulus clouds), to about 0.25 g m^{-3}.~~ The relatively low N_c in the KAPPA, SAT0.2 and SAT1.0 simulations is the direct result of prohibiting 'repeated activation' as discussed above in Sect. 2.1.1. With the absence of additional in-cloud activation, droplets only activate at cloud base and are distributed over the whole cloud, leading to low N_c. Although in-cloud activation is allowed in the PN simulation, the governing equation also severely limits how much of the available aerosol is activated. Both simulations show a decrease of N_c with altitude as most activation takes place near cloud base.

Simulated cloud liquid water content q_c increases with the calculated or assumed N_c. The BASE simulation ~~clearly overestimates~~ has the highest (fixed) value of N_c and simulates q_c with a continuous increase up to 1.5 g m^{-3} at 2500 m altitude. The BASE30 simulation shows a similar profile up to an altitude of 1500 m. From there to cloud top, q_c is considerably lower, ~~but still too high~~ with values around 0.7 g m^{-3}. ~~Despite the underestimation of N_c, the KAPPA simulation shows a striking agreement with the observations for q_c.~~ The PN simulation follows the BASE and BASE30 simulations up to ~~1100~~ 1200 m, but levels off at values around 0.4 g m^{-3}.

~~While the observations show that the characteristics of the clouds are fairly well constrained, values for precipitation show considerably more spread. Hence, a logarithmic scale is used for both N_r and q_r. Observations indicate values of N_r around 1 dm~~The KAPPA simulation diverges from the other simulations as it levels off at 0.25 g m^{-3} ~~up to 1000m, increasing to 10 dm^{-3} at 2000m and even higher above. These values are captured well by~~ . In comparison, observations of the ~~BASE simulation, although simulated surface values are too low. The BASE30 simulation calculates higher N_r values at all altitudes, especially in the upper half of the cloud layer. In the KAPPAsimulation, values for N_r are substantially higher than the observations. Surface values are correctly simulated at 1 dm~~RICO campaign show a somewhat slower continuous increase with height (as expected for shallow cumulus clouds), to about 0.25 g m^{-3} ~~, but increase to 100 dm^{-3} in the lower parts of the cloud layer around 1000 m. From there, N_r shows a steady increase to 350 dm^{-3} at the top of the cloud layer~~ around 1250 m and above. ~~Note the stark contrast of the overestimation of N_r combined with an underestimation of N_c. The vertical profile in~~

Above-mentioned differences in q_c are accompanied by substantial differences in domain-averages in liquid water path (LWP). Consistent with q_c the BASE and BASE30 simulations calculate the highest LWP: 11.36 and 11.09 g m^{-2} respectively. The lowest LWP is simulated by KAPPA: 4.43 g m^{-2}, while PN has an average LWP of 8.81 g m^{-2}. The relative differences in LWP are larger than q_c because the simulations also differ in average cloud fraction. When considering actual volume occupied by clouds (i.e. $q_c > 0.01$ g kg^{-1}) in the cloud layer between 500 and 2000 meter BASE and BASE30 are again highest and relatively similar: 2.04 and 2.07%. KAPPA deviates most from this and calculates 1.58%. In the PN simulation ~~resembles the profile found in BASE/BASE30, albeit with higher values .~~ this is 1.97%.

While the observations of the cloud characteristics are fairly well constrained, values for precipitation show considerably more spread. Hence, a logarithmic scale is used for both N_r and q_r. Observed rain water content q_r fluctuates greatly with median values between 0.001 and 2 g m^{-3}.

Simulated values show more stable values and smoother profiles. Simulations with the highest q_c show the lowest values for q_r. The BASE simulation ~~underestimates~~ calculates values for q_r ~~with values~~ of about 0.0025 g m^{-3} up to an altitude of ~~1500m~~1500 m, above which the values increase with height to 0.03 g m^{-3} at ~~2300m~~2300 m. The BASE30 simulation shows a ~~better agreement with observation with calculated values~~ substantially higher amount of rainwater in the lowest lowest 1100 m with a median of about 0.006 g m^{-3}~~in the lowest 1100 m and from there~~. From there q_r increases to 0.01 g m^{-3} at 2000 m altitude. In the KAPPA simulation q_r is similar to the BASE30 simulation near the surface. However, in KAPPA q_r shows a sharp increase between 500 and 600 m followed by gradual increases to 0.01 g m^{-3} at 2000 m. The PN simulation shows a similar profile, with the sharp increase located around ~~1000m~~1000 m to the same value of 0.01 g m^{-3}.

Observations indicate values of N_r around 1 dm^{-3} up to 1000 m, increasing to 10 dm^{-3} at 2000 m and even higher above. The BASE simulation shows the lowest values for N_r, in accordance with q_r. From 10-100 dm^{-3} at the surface, N_r continuously increases to 10-100 dm^{-3} at the cloud tops. The BASE30 simulation calculates higher N_r values at all altitudes, especially in the upper half of the cloud layer. In the KAPPA simulation, values for N_r are substantially higher. Surface values are around 1 dm^{-3}, but increase with a much steeper slope to 100 dm^{-3} in the lower parts of the cloud layer around 1000 m. From there, N_r shows a steady increase to 350 dm^{-3} at the top of the cloud layer. Note the stark contrast of high values for N_r combined with low values of N_c. The vertical profile in PN is in between the BASE/BASE30 and the KAPPA simulations. It resembles the profile found in BASE30, albeit with higher values.

The differences in q_c and and precipitation are all related to the simulated (or prescribed) cloud droplet concentration N_c. The initial conditions (i.e. total water content and temperature) under which the clouds form are the same in all simulations. By decreasing N_c, the ~~same water is thus~~ liquid water is distributed over less droplets leading to larger cloud droplets. This leads to a faster ~~formation of rain~~ rain formation as the droplets ~~reach a size at which they are transformed into precipitation~~ grow more quickly. From a macrodynamic perspective, a lower N_c decreases the water holding capacity of a cloud. This is reflected in the profiles of q_c. Near cloud base all simulations show the same q_c, but in the KAPPA and PN ~~simulation~~ simulations the water holding capacity is reached and all excess water is transformed into precipitation. This level is maintained in the rest of the cloud layer. In the BASE and BASE30 simulations, this limit ~~mighty not be~~ is not reached and q_c keeps increasing throughout the cloud layer. Another interesting result is that a decrease in N_c leads to an increase in N_r (reversed order of the simulations in the first and third panel of Fig. 4). The cloud droplets in the KAPPA simulation (and to a somewhat lesser extent in the PN simulation) are so large that collision-coalescence of cloud droplets quickly results in rain size droplets (i.e. autoconversion). In the BASE and BASE30 simulations, the cloud droplets are smaller and more collisions are needed to form raindrops. Indeed, we find that the strength of autoconversion is higher in the KAPPA and PN simulations than in the BASE and BASE30 simulations and takes place at lower altitudes (not shown). In the BASE and BASE30 simulations, most rainwater is gained through the collection of cloud droplets by falling raindrops (accretion).

None of the simulations scores best on all metrics. Our new aerosol framework (KAPPA) scores exceptionally well for q_c, but underestimates N_c and calculates too much precipitation. If we do set A full validation and direct comparison of the simulation results with observations would require inputs derived from collocated observations of both aerosol size distributions and composition as well as an elaborate investigation of the influence of model set-up, i.e. convergence of results regarding model resolution and domain size (e.g. Matheou et al., 2011). Nevertheless, it is noteworthy that the KAPPA simulation with the lowest N_c to values corresponding to best resembles the observed q_c, while setting N_c to the observed values in the BASE30 simulation , results in an overestimation of q_c. In our framework, N_c can no longer be adjusted to improve the simulated values of q_c are overestimated. Howeverthe other cloud microphysical properties, but follows from the aerosol population and calculated thermodynamics. In this way, the results of our framework can act as a starting point for further improvement of the numerical implementation of the microphysical processes. Possible pathways for improvement are discussed in Sect. 4.

3.2 Aerosol microphysics

3.1.1 Aerosol microphysics

In this section we focus on the feedback of ACI on the aerosol population by discussing changes to aerosol population as a result of cloud microphysical processes. Here, we discuss the results of the KAPPA and PN simulations. As shown above, the different numerical descriptions of activation (Sect. 2.1.1) cause substantial differences in the cloud and rain characteristics. This, in turn, yields differences in the feedback to the aerosol population. A comparison between the two simulations provides insight into the network of the different microphysical processes and the overall impact on the aerosol distribution.

Section 3.1.2 describes the influence of the different microphysical processes to the bulk properties of the aerosol (i.e. domain average of the aerosol mass) and the resulting vertical profiles of aerosol mass and number at the end of the simulation. Section 3.1.3 subsequently describes effects of ACI focusses on the aerosol size in more detail. This is done by comparing the typical aerosol size associated with the different microphysical processes (i.e. typical aerosol size after resuspension from raindrops compared to the initially activated aerosols).

3.1.2 Contribution of individual processes to the aerosol budget

The effective influence of the different microphysical processes on the five aerosol species is shown in Tables 3 and 4 for the KAPPA and PN simulation respectively. The values are scaled to the species-specific total mass and thus can be interpreted as a processing timescale.

3.1.3 Contribution of individual processes to the aerosol budget

The effective influence of the different microphysical processes on the five aerosol species is shown in Tables 3 and 4 for the KAPPA and PN simulation respectively. The values are scaled to the species-specific total mass and thus can be interpreted as a processing timescale. The in-cloud aerosol mass has two source processes: activation and in-cloud scavenging by cloud droplets, displayed in the first two columns of Tables 3 and 4. For both simulations, we find that virtually all in-cloud aerosol

Table 3. Domain-average total column microphysical process strengths (kg kg^{-1} day^{-1}) in the KAPPA simulation for the different aerosol species. All values are scaled to , divided by the species total column aerosol mass (kg kg^{-1}) and rescaled to have the unit day^{-1}. Reported values can be thus interpreted as timescales(day^{-1}). For example, e.g. activation processes 1.37 1.36 times the total column sea salt aerosol mass per day.

	activation	in-cloud scavenging	cloud evaporation	cloud-to-rain conversion	rain scavenging	rain evaporation	rain sedimentation
Sea salt	1.37 1.36	1.09×10^{-2}	1.19 1.18	0.21	2.35 2.30	1.30	1.30 1.25
Sulphate	0.70	$3.413.46\times10^{-3}$	0.60 0.61	0.11	0.90 0.89	0.56	0.46 0.45
Organic matter	0.44	$2.162.20\times10^{-3}$	0.38	0.07	0.56 0.55	0.35	0.28
Black carbon	0.52	$2.612.65\times10^{-3}$	0.45	0.08	0.62	0.39	0.32 0.31
Mineral dust	0.37	$2.802.83\times10^{-3}$	0.32	0.06	0.61 0.60	0.37 0.38	0.30 0.29
Water						$3.513.60\times10^{-2}$	$2.522.62\times10^{-3}$

Table 4. Same as Table 3, but for the PN simulation.

	activation	in-cloud scavenging	cloud evaporation	cloud-to-rain conversion	rain scavenging	rain evaporation	rain sedimentation
			17.89				
Sea salt	18.62 18.0	$2.332.41\times10^{-4}$	17.40	0.70 0.74	1.65 1.70	0.96 0.97	1.44 1.47
Sulphate	10.00 9.70	$1.221.24\times10^{-4}$	9.59 9.34	0.40 0.41	0.73 0.75	0.51	0.64 0.65
Organic matter	6.25 6.06	$1.451.46\times10^{-4}$	6.00 5.84	0.25 0.26	0.45 0.47	0.32	0.40 0.41
Black carbon	7.11 6.89	$3.823.83\times10^{-4}$	6.82 6.64	0.28 0.29	0.52 0.53	0.36	0.45 0.46
Mineral dust	5.24 5.07	$1.481.54\times10^{-3}$	5.03 4.89	0.21 0.22	0.50 0.52	0.33	0.39 0.40
Water						$1.942.02\times10^{-2}$	$2.512.60\times10^{-3}$

mass (> 99%) is gained through activation while in-cloud scavenging of interstitial aerosol is negligible. The relatively low values for N_c lead to rather ineffective in-cloud scavenging.

Most of the in-cloud aerosol mass is resuspended to the atmosphere after evaporation of cloud droplets carrying the aerosol. In the KAPPA simulation ~8587% of the in-cloud aerosol is resuspended, while in the PN simulation this 'cloud evaporation fraction' is ~96%. This difference in cloud cycling is a direct result of the difference in The activation scheme in the PN simulation activates more aerosol and thus calculates higher N_c between the two simulations as can be seen in Fig. 4, panel (a). In PN, the same cloud water is distributed over more but smaller cloud droplets. . This delays precipitation formation which is reflected in higher q_c in clouds, higher LWP and cloud fraction as discussed in Sect. 3.1.1. Consequently, less cloud droplets grow large enough to form rain and are aerosol is removed from the atmosphere by precipitation and resuspended when the

cloud evaporates ~~. As a result, more aerosol mass remains in the atmosphere to be incorporated in a subsequent cloud cycle.~~ instead.

Corresponding aerosol fluxes for activation and cloud evaporation are ~~12-13~~ 13 times larger in PN compared to KAPPA, i.e. in the PN simulation clouds process a total of ~~18.62~~ 18.0 times the available sea salt aerosol mass per day instead of ~~1.37~~ 1.36 when using the KAPPA activation. Due to the large cloud evaporation fraction the large activation flux does not directly lead to a similar increase in cloud-to-rain conversion of aerosol. Instead, we find that conversion is 'only' ~3.5 times stronger in the PN simulation compared to the KAPPA simulation (e.g. conversion of the available sea salt mass: ~~0.70~~ 0.74 day^{-1} in PN vs. 0.21 day^{-1} in KAPPA).

The strength of interaction between aerosol and clouds differs greatly between aerosol species. For example, the processing rate of sea salt by cloud activation (~~1.37~~ 1.36 day^{-1} in KAPPA) is 2.6 times larger than for mineral dust (0.52 day^{-1} in KAPPA). As expected, the most hygroscopic species are most susceptible to the activation process. However, note that the combination of the different species within a lognormal mode of the aerosol framework determines the activation for that mode (see Sect. 2.1.1). As a result, organic matter is processed more slowly than black carbon despite the higher hygroscopicity of this species. Because the simulated case is over the ocean and relatively remote, species like black carbon have aged significantly and mainly reside in the accumulation mode. Therefore it is activated alongside the highly hygroscopic sea salt aerosol in the accumulation mode. The differences in the rates for resuspension after cloud evaporation and cloud-to-rain conversion closely follow those of the activation process. This is caused by the fact we assume an internal aerosol mixture of the in-cloud aerosol mass. Cloud processes thus act similar on the aerosol species as soon as they are incorporated in cloud droplets.

Besides cloud-to-rain conversion, falling precipitation gains additional aerosol mass by rain scavenging. In fact, this process is the dominant source for in-rain aerosol mass. Comparing the process strengths in the KAPPA simulation of cloud-to-rain conversion (e.g. 0.21 day^{-1} for sea salt) and rain scavenging (~~2.35~~ 2.30 day^{-1} for sea salt), we find that ~~õ90~~89-91% of the in-rain aerosol mass is gained by falling precipitation. This is a direct result of the high q_r in this simulation. The lower q_r in the PN simulation (see Fig. 4) corresponds to a lower scavenging by precipitation. With a relative contribution of ~~65-70~~64-70% it remains the most dominant source process for in-rain aerosol mass. Interestingly, cloud-to-rain conversion and scavenging together process a relatively similar amount of aerosol mass in both simulations.

Once the aerosol is incorporated in rain, it can be removed from the atmosphere by sedimentation (rain-out) or it can be resuspended upon evaporation of the rain drops, shown in the last two columns of Tables 3 and 4. The strength of these two processes is about the same. In the KAPPA simulation, ~~50-55~~51-56% of the aerosol mass is resuspended by evaporating rain, while in the PN simulation this is ~~40-46~~40-45%. This difference is again linked to the slower rain water formation in the PN simulation (i.e. smaller N_r, see Fig. 4). Less cloud drops are transformed to rain, which are on average larger and thus less prone to evaporate. Because the aerosol mass is only released upon complete evaporation of a rain, this leads to a lower evaporating fraction. The precipitation rate (i.e. water that reaches the surface) is the same in both simulations (see Table 3 and 4 as well as Fig. 4). This leads to a removal of aerosol in the PN simulation that is ~~10-40%~~ 17% (sea salt) to 48% (black carbon) higher than in the KAPPA simulation.

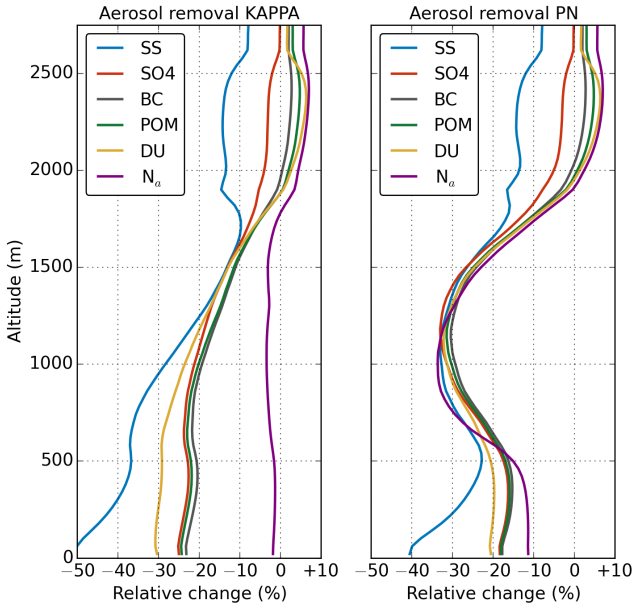

Figure 5. Vertical profile of domain-averaged aerosol mass and number concentration after 6 hours for the KAPPA (left) and PN (right) simulations relative to the initial profile.

~~When comparing the abovementioned ratios of resuspension-to-sedimentation of~~ The above-mentioned balance between the two sink processes for in-rain aerosol ~~to the rainwater itself, we find that this ratio is considerably smaller than for rainwater.~~ (i.e., resuspension vs. sedimentation) is substantially different than for the rainwater itself. In the KAPPA simulation, 93~~or 83% evaporates instead of reaching the surface in the KAPPA and PN simulations respectively.~~ % of the falling precipitation evaporates which leads to the resuspension of only 51-56% of the in-rain aerosol mass. A similar ratio is found in the PN simulation: 86% evaporated rainwater vs. 40-45% resuspended aerosol. As explained in Sect. 2.1.4, the fraction of released aerosol mass is always lower than the fraction of evaporated rain water. However, the disparity exceeds the correction of Gong et al. (2006) because below the cloud, falling precipitation keeps gaining additional in-rain aerosol through scavenging, whereas the amount of water only decreases.

The combination of the microphysical processes discussed above leads to the ultimate removal of aerosol shown in Fig. 5. ~~In the KAPPA simulation~~ Total column aerosol mass at the end of the simulation has decreased 24% in the KAPPA simulation and 21% in the PN simulation. The two simulations show different vertical profiles of the remaining aerosol, which is the ~~removal is strongest near the surface and decreases with height. In this~~ result of the different balance between microphysical described processes above. In the KAPPA simulation, rain scavenging was found to account for about 90% of the in-rain aerosol. Consequently, the ~~vertical profile of the aerosol removal from the atmosphere is mostly determined by this process. Because rain scavenging acts on both the cloud and below-cloud layer, removal is relatively homogenous in the vertical~~the

removal is strongest near the surface and decreases with height. The small local maximum around 400 m reflects evaporation of precipitation below the cloud base, while the zone of activation at the cloud base is visible in the local minimum around 600 m.

When using the PN activation scheme, aerosol removal and the governing processes change considerably. The importance of cloud-to-rain conversion for the in-rain aerosol mass increases in the PN simulation compared to KAPPA. Consequently, aerosol removal in the cloud layer ~~increased up to~~ is enhanced by -30%. In contrast, net removal below the cloud layer decreased as a result of resuspended aerosol mass originating from the cloud layer.

The decrease in aerosol number is substantially different between the KAPPA and PN simulation. While the reduction in aerosol number in KAPPA is limited (< 3%), the PN simulation calculates removal of aerosol number up to -34%. The dominant removal by rain scavenging in the KAPPA simulation is most effective for large particles and thus results in the removal of the largest particles. Moreover, when droplets evaporate, the smallest droplets evaporate first and thus resuspend the smallest aerosols first since the aerosol mass in rain is distributed homogeneously over all available rainwater. This further increases the tendency for large particles to be removed from the atmosphere. The resulting removal of aerosol number in the KAPPA simulation is therefore much smaller than the removal in aerosol mass. In the PN simulation, aerosols are cycled through the clouds more frequently. Due to collision-coalescence of cloud droplets, resuspended aerosols will be larger than the initially activated particles. This results in removal of aerosol number in the cloud layer, but has no effect on aerosol mass.

The behaviour of the different aerosol species is similar in the PN and KAPPA simulations and mainly determined by the typical aerosol particle size because the effectivity of scavenging as well as activation increases with aerosol size. The largest decrease is found for sea salt, followed by mineral dust. Profiles of sulphate, organic matter and black carbon are similar and display the weakest removal. The vertical profile for sea salt stands out due to the vertical distribution of this species, which decreases strongly with height (see Fig. 2). The concentrations of the other species are relatively constant with altitude. Due to this, resuspension of sea salt aerosol brought down from the cloud layer is not sufficient to replenish the sea salt aerosol scavenged by falling precipitation close to the surface.

3.1.3 Changes in the aerosol size distribution

Analysis of the remaining aerosol ~~population~~ total mass and number in the previous Sect. 3.1.2 already indicates that changes in the cloud characteristics might cause substantial differences in ~~how ACI feeds back to the aerosol characteristics~~the cloud processes influence the aerosol size distribution. To better quantify this cloud processing, the following section will compare the median radius for particles associated with the different microphysical processes.

An overview of the typical aerosol median radius associated with the cloud and rain microphysical processes is shown in Table 5. At the beginning of a cloud cycle, we find an average median radius of activated aerosols of ~~134~~ 132 nm in the cloud layer (between 500 and 2000 m) in the KAPPA simulation. In the PN simulation this radius is ~~191.7~~ 192 nm. This

Table 5. Typical dry aerosol median radius (nm) associated with the microphysical processes for the KAPPA and PN simulations

	KAPPA	PN
In the cloud layer (500 - 2000 m)		
Activation	~~133.8~~ 132	~~191.7~~ 192
In-cloud scavenging	~~76.6~~ 76	~~10.2~~ 10
Cloud-to-rain conversion	~~175.9~~ 174	~~275.2~~ 275
Cloud evaporation	~~141.4~~ 140	~~210.6~~ 210
Rain scavenging	~~632.6~~ 631	~~596.0~~ 595
Rain evaporation	~~454.2~~ 456	~~813.1~~ 794
Below the cloud layer (0 - 500 m)		
Rain scavenging	~~677.0~~ 675	~~701.1~~ 701
Rain evaporation	~~1651.0~~ 1649	~~2929.0~~ 2909
Rain sedimentation	~~1861.8~~ 1838	~~3598.6~~ 3570

increase of ~~43~~45% is caused by the substantially stronger cycling of aerosol through the clouds in the PN simulation. Inside the clouds, droplets are merged into larger droplets by collision-coalescence. When these cloud droplets evaporate, larger and less numerous aerosol particles are resuspended to the atmosphere. Because a larger fraction (compare Tables 3 and 4) of the cloud droplets are actually resuspended to the atmosphere in the PN simulation, this 'cloud processing' has a stronger effect on the aerosol population.

Additionally, the higher evaporation fraction in the PN simulation also has a direct influence on the size of the resuspended aerosols. As explained in Sect. 2.1.4 aerosols are only resuspended when a droplet completely evaporates. Because the smallest droplets evaporate first, the smallest incorporated aerosols are also resuspended first, since the aerosol concentration is homogeneously distributed over the hydrometeor size distribution. When the evaporation fraction increases, larger droplets can evaporate completely increasing the average resuspended aerosol size. In the KAPPA simulation, resuspended aerosol particles resulting from cloud evaporation are ~~5.7~~6% larger (~~141~~ 140 nm) than the initially scavenged aerosols. In the PN simulation, the resuspended aerosols are ~~9.8~~9% larger (~~210.6~~ 210 nm).

Interstitial aerosols scavenged by cloud droplets are substantially smaller than the activated aerosols as the largest particles have been activated. In the KAPPA simulation the typical radius is of scavenged interstitial aerosol is ~~77~~ 76 nm, compared to ~~10.2~~ 10 nm in the PN simulation. The activation scheme in the PN simulation activates a larger amount of particles, leaving

even less interstitial aerosol for in-cloud scavenging. In both simulations, in-cloud scavenging is relatively weak and has no substantial influence on the typical aerosol size associated with the other processes.

The cloud-to-rain converted droplets contain aerosols with a median radius of ~~176~~ 174 nm, which is ~~31~~32% larger than the activated aerosol in the KAPPA simulation. In the PN simulation, the relative size of aerosols involved in cloud-to-rain conversion is ~~275.2~~ 275 nm (+43%). This increase in aerosol size is again linked to the higher cloud evaporation fraction. Higher cloud evaporation allows larger droplets to evaporate completely, but the largest ones still remain and are converted to raindrops. In fact, by now evaporating more droplets, conversion is further shifted towards the large-end tail of the cloud droplet size distribution. Consequently, the typical aerosol radius for cloud-to-rain conversion increases together with the typical radius for resuspension.

Due to the strength of rain scavenging in the simulations, in-rain aerosol mass grows considerably. As a result, raindrops evaporating in the cloud layer produce aerosols with a median radius of ~~454~~ 456 nm in the KAPPA simulation. In the PN simulation, the average aerosol radius associated rain evaporation is ~~813.1~~ 794 nm. This difference is caused by the fact that the rain water and in-rain aerosol mass is distributed over fewer and therefore larger raindroplets in the PN simulation. This leads to a direct increase of the typical aerosol size associated with the evaporation of precipitation.

The average median radius of the aerosol particles scavenged by falling precipitation is ~~633~~ 631 nm in the cloud layer in the KAPPA simulation. Note that this exceeds the typical median radius for evaporated aerosols. The preference for scavenging to remove the largest particles still plays a role for aerosols of this size, i.e. rain scavenging is an order of magnitude more effective for mass than number (Croft et al., 2009, their Fig. 1).

Below the cloud layer (<~~500m~~500 m), falling precipitation has had more time to collect aerosol mass. Additionally, outside the cloud the evaporation fraction is substantially higher. This leads to a considerable increase in the size of the resuspended aerosols. In the KAPPA simulation, the typical median aerosol radius is 1.65 µm, ~~12.3~~ 12.5 times larger than the initially activated aerosols. The average size of the resuspended aerosols in the PN simulation is ~~2.92~~ 2.91 µm. This is an even stronger increase of ~~15.3~~ 15.2 times the size of the originally activated aerosols. Note that these large resuspended aerosols are prone to sedimentation, a process that has been left out of the current simulations.

To summarize, the results of the KAPPA and PN simulations illustrate that the influence of ~~ACI~~ cloud processing on the aerosol size distribution depends on how much of the in-cloud and in-rain aerosol is ultimately removed. Due to collision-coalescence of cloud droplets, aerosol mass is redistributed over fewer droplets. Complete evaporation of these droplets would release aerosol particles larger than those originally activated and scavenged. However, when the clouds produce precipitation, the largest cloud droplets containing most aerosol mass are the droplets most likely to be converted to precipitation and to be removed from the atmosphere. Subsequent evaporation of the remaining droplets then also leads to a decrease of the average aerosol size. It thus depends on the balance between evaporation fraction and precipitation, whether the average size of the resuspended aerosols is larger or smaller than the initially activated aerosols. With a high evaporation fraction, fewer droplets are transformed to rain and these contain larger aerosols on average. Additionally, when precipitation is formed,

scavenging of aerosols by falling precipitation adds a substantial amount of aerosol mass to the rainwater. The aerosols released by evaporation of these raindrops increase the average aerosol size considerably.

4 Discussion

The aerosol framework now implemented in the DALES model is specifically designed to gain insight in the aerosol-cloud interaction ~~and particularly the effect of aerosol-cloud interaction~~ interactions and the effect on the aerosol population in particular. By incorporating aerosols into the modelling framework and coupling it to the cloud microphysics, there is no longer a need for assumptions on how cloud characteristics change due to changes in the aerosol population. Instead, measured (or modelled in large scale models) aerosol concentrations can be used to calculate corresponding cloud characteristics. An important feature of the aerosol framework is the ability to simulate multiple aerosol species, so that aerosol activation can be based on the aerosol characteristics in a fundamental way, i.e. through κ-Köhler theory. Moreover, the effect of ACI on the aerosol population can be determined for individual aerosol species.

However, this increased complexity requires additional validation of the simulated aerosol population. To better constrain model results, there is particular interest in collocated cloud and aerosol measurements in, next to, and below clouds. Examples of recent campaigns collecting this type of measurements are GoAmazon2014/5 (Martin et al., 2017) and DACCIWA (Flamant et al., 2018). Observations of both aerosol size distribution and chemical composition are invaluable to the level of detail we pursue here. Measurements of aerosols near cloud-base in combination with N_c provide insight in the process of activation. ~~Processing of the aerosols by ACI~~ Cloud processing of aerosols can be investigated by determining the aerosol characteristics near cloud edges or at the location of dissipating clouds. Additionally, measuring aerosols in the wake of a precipitation zone allows for the validation of the effect of rain scavenging and evaporation of precipitation on the aerosol population. As discussed in Sect. 3.1.3, the original simulation length of vanZanten et al. (2011) was shortened from 24 to 6 hours to avoid a too strong depletion of the aerosol population by wash-out. This would let the simulations diverge too much from the original case and decrease the already low simulated N_c and strengthen the rain formation at the expense of clouds forming and evaporation without precipitation.

Including aerosol emission and chemical formation to sustain aerosol levels would facilitate longer simulations. However, without observation-based constraints on these processes this would introduce additional uncertainty and partly negate the goal of this work to have a model that includes both sides of ACI: the effect of aerosols on cloud and vice versa. Simulated N_c would be a direct result of the chosen emission strength, basically going back to the BASE simulations in which N_c is prescribed.

The exploratory analysis performed in this work only considered domain average values of the clouds and aerosol. However, the richness of LES modelling allows for a deeper understanding of the aerosol-cloud ~~interaction~~interactions. Translating model data into quantitative results that do justice to the resolved complexity in LES simulations requires more comprehensive techniques. For example, convective cell tracking described in Heikenfeld et al. (2019) enable this kind of research by tracking of individual clouds and averaging their statistics.

The introduction of aerosols puts increased demands on the numerical implementation of the cloud microphysical processes as well. Sect. 3.1.1 showed a trade-off between correct simulation of N_c or q_c. Because the aerosol population now determines the cloud characteristics, a previously prescribed value like N_c can no longer be adjusted to improve model results. Especially cases like the RICO campaign (with a pristine environment and low values for N_c) might reveal issues that were previously hidden. At the same time, combined with detailed observations, our framework is an excellent starting point to improve the microphysics parameterization in LES models. Parameters of the microphysics framework that might strongly influence the model outcome are (1) the radius that separates cloud from raindrops and (2) the parameters that describe the size distribution of the hydrometeors. Moreover, processes like autoconversion and accretion, as well as cloud droplet self-collection do not depend on N_c in the current numerical implementation of the cloud microphysics in DALES. A well-validated case of both aerosol and cloud characteristics could provide a good starting point to evaluate the accuracy modelled microphysical processes and its sensitivity to these critical parameters.

~~While the default value for N_c in the BASE version of DALES is a substantial overestimation compared to observations, the simulations with the new framework calculate values below the observed N_c. Moreover, the relatively small~~ The difference in N_c between the KAPPA and PN simulations ~~yielded large differences for~~ translated into substantial differences in the resulting aerosol population. ~~This~~ In fact, this difference in N_c is part of a more general issue on how to numerically address the microphysical process of aerosol activation. The number of activated aerosol particles is largely determined by the maximum value of supersaturation near cloud base (e.g. Derksen et al., 2009). Supersaturation is the result of the balance between the source of available moisture resulting from the dynamics and the sink of moisture by condensation on aerosols and cloud droplets. Currently, DALES uses a diagnostic description of cloud liquid water and a fixed value for supersaturation. Although this gives a strict limitation to which aerosols can grow to cloud droplets, the modal aerosol framework does not allow this sharp cut-off in the size distribution. In subsequent timesteps, aerosol mass and number are redistributed within the lognormal modes. Consequently, a part of the large-end tail of the size distribution is considered to be large enough to activate each timestep. This results in a 'runaway' activation yielding unrealistic $N_c > 200$ cm^{-3} (not shown). This problem was also recognised in Pousse-Nottelmann et al. (2015), but the PN activation scheme limits activation by subtracting the number of existing cloud droplets N_c from the calculated amount of newly activated aerosols. Furthermore, a hard limit is set by only allowing particles larger than 35 nm to activate. A complete solution to this problem would be to use a sectional or bin approach to describe the aerosol population, which does allow changes to the shape of the size distribution and thus a sharp cut-off that results from activation. However, this flexibility comes with high computational cost; especially with a focus on the chemical composition of the aerosol population and the inclusion of multiple aerosol species (e.g. Kurppa et al. (2019), Table 2). A future improvement to DALES would be to replace the diagnostic calculation of cloud water by a prognostic variable. Supersaturation and activation can then be calculated interactively and be determined by the balance between available moisture resulting from the dynamics and available surface of aerosol and existing cloud droplets to condense on.

In Sect. 3.1.1, the comparison between the KAPPA and PN simulations illustrated important aspects of the interaction between aerosol and clouds. Here, we found an interesting competition between growth of aerosols through cloud processing and

removal of the largest particles by precipitation. Future research could investigate the mechanisms that determine the balance between processing and removal. Settings like the pristine ocean of the RICO campaign alone might not be suitable for this as the low values of N_c inherently lead to rapid formation of precipitation and strong scavenging by falling precipitation. Simulations with higher aerosol burden and different meteorological settings should be used to investigate a large range of different cloud regimes.

5 Conclusions

The implementation of an explicit aerosol framework is a step forward in the simulation of aerosol-cloud ~~interaction~~ interactions in the DALES model (Heus et al., 2010; Ouwersloot et al., 2017) as we can now quantify the feedback of the cloud microphysics on the aerosol population. Moreover, the aerosol module M7 (Vignati et al., 2004) represents an external mixture of multiple aerosol species. This allows an explicit and more fundamental approach to calculating aerosol activation by using κ-Köhler theory (Petters and Kreidenweis, 2007). Evaluation for the Rain in Shallow Cumulus over the Ocean (RICO) campaign (Rauber et al., 2007), showed that DALES reproduces the precipitating shallow cumulus clouds typical for this case. ~~A trade-off exists in the correct simulation of cloud characteristics as the new aerosol framework leads to a better simulation of q_c, resulting from an underestimation of N_c, regardless of the activation scheme.~~

After evaluation with the RICO observations, our framework has been used to explore the feedback of aerosol-cloud ~~interaction~~ interactions on the aerosol population. The main findings of this study are:

1. In the clean background atmosphere, virtually all in-cloud aerosol mass is gained through activation regardless of the activation scheme. In-cloud scavenging is inefficient at the low simulated cloud droplet concentrations. Despite the relatively rapid formation of precipitation, only 5-15% of the aerosol mass is converted to rain.

2. Most of the in-rain aerosol mass is gained through scavenging by falling precipitation. It is the most dominant removal process of aerosol (mass) from the atmosphere. For the aerosol mass incorporated in rain, resuspension after evaporation of falling precipitation is of similar magnitude as the aerosol mass removed from the atmosphere by precipitation reaching the surface. This is in stark contrast to the evaporation/sedimentation ratio of rain water, of which only ~10% reaches the surface in our simulations.

3. The strength of aerosol-cloud interaction differs considerably between aerosol species. Timescales associated with the ultimate removal of aerosol by sedimentation range from almost 4 days for organic matter to less than a day for sea salt. For water, the timescale is even slower due to the strong evaporation of precipitation caused by the meteorological conditions in RICO.

4. The change in aerosol radius between activated aerosol and aerosol resuspended from evaporated cloud droplets is found to be relatively small (5-10%). In contrast, the median radius of aerosols released by evaporating precipitation is an order of magnitude larger than the initially scavenged aerosol.

Future research will focus on ~~further~~ evaluation of the M7-DALES framework under more polluted regimes in which cloud processing of the aerosol population may differ substantially. Additionally, further development includes the implementation of M7 aerosol microphysical processes (e.g. coagulation) and ~~coupling to chemical processes~~inclusion of aqueous-phase oxidation of dissolved (gaseous) species. The diagnostic approach to cloud water will be replaced by a prognostic calculation to incorporate the interaction between aerosols and clouds through changes in supersaturation.

6 ~~Code and data availability~~

~~The DALES source code is available on https://github.com/dalesteam/dales (last access: 13 May 2019). The distribution is under the GNU General Public License v3. The exact version used in this work DALES4.1-M7 and case-specific input files can be downloaded from http://doi.org/10.5281/zenodo.3241356.~~

Code availability. The DALES source code is available on https://github.com/dalesteam/dales (last access: 13 May 2019). The distribution is under the GNU General Public License v3. This line of development of DALES is currently in progress and still an unfinished research line. After completion, we intend to merge this branch into the main DALES repository. The exact version used in this work DALES4.1-M7 and case-specific input files can be downloaded from http://doi.org/10.5281/zenodo.3241356.

6 ~~Aerosol initialisation~~

~~Initial vertical profiles of aerosol mass concentration (g kg^{-1}) of (a) sulphate, (b) black carbon, (c) particulate organic matter, (d) sea salt, (e) mineral dust and (f) number concentration (kg^{-1}) extracted from the TM5mp model (Bergman et al., 2019). Aerosol modes are specified by different colors which are consistent between panels. Circles correspond to the TM5mp model levels. Note the break in the horizontal axis in panel (c).~~

~~Necessary observations of aerosol vertical profile and composition are not available from the RICO campaign. Instead, TM5mp (Williams et al., 2017; Bergman et al., 2019) output is used to initialise the aerosol scalar fields. The simulations were originally carried out for a remote sensing experiment for the Aerocom project (http://aerocom.met.no) by the Dutch Meteorological Institute (KNMI) in 2017. Because this simulation period did not include the duration of the RICO campaign period, an average is constructed using profiles of December 1st for the years 2006, 2008 and 2010.~~

~~Since TM5mp uses the same modal aerosol framework M7, a one-to-one translation of the aerosol scalar fields can be made. The only difference between the latest version of TM5 (Bergman et al., 2019) and DALES in the aerosol representation is the inclusion of secondary organic aerosol in the TM5mp model. This is expressed in the presence of POM in the soluble nucleation (NUS) mode which does not exist in DALES. The corresponding mass is negligible, but is incorporated in the POM Aitken soluble (AIS) mode mass nevertheless.~~

~~The TM5mp output is provided on native model pressure fields.These pressure fields are transformed to altitude coordinates using corresponding temperature fields. Since our simulations concern a case over the ocean, no corrections for topography are~~

needed. The resulting transformation yields 9 levels in the lowest 5000 m, which is the vertical extent of the DALES model simulations. Of these pressure levels, 4 are located near the surface (i.e. below 1000 m). Linear interpolation is used between these levels and the values between top and bottom of DALES gridboxes are averaged and assigned to the DALES vertical grid. Resulting profiles are shown in Fig. 2.

As expected for the ocean region of RICO, 90% of the aerosol mass consists of sea salt particles. The sea salt mass concentration in the lowest 2000 m is 10.0 g m^{-3}. The other species account for 0.69 g m^{-3} (sulphate), 0.19 g m^{-3} (mineral dust), 0.14 g m^{-3} (organic matter) and 0.027 g m^{-3} (black carbon). Additionally, the sea salt mass concentration shows a decrease with height, explained by the fact that it is locally generated. The concentrations of the other species are more or less constant with height or even show a slight increase with height. For the pristine environment in the RICO campaign, these species are advected into the region and display characteristics of an aged aerosol population. For example, the mineral dust particles are considerably smaller than the sea salt particles and mainly reside in the soluble modes.

The total number concentration in the lowest 2000 m is 202 cm^{-3}, mainly consisting of Aitken mode particles (149.6 cm^{-3}). Of all aerosol particles, 82.59 cm^{-3} activate at a supersaturation of 0.4%. This value is diagnosed by applying the κ-Köhler theory with the characteristic values of the different species shown in Table 1.

Author contributions. MdB and MK set up the research. MdB implemented the code in DALES and carried out the simulations. MdB interpreted the data and prepared the manuscript with comments and contributions from all co-authors.

Competing interests. The authors declare that they have no conflict of interest.

Acknowledgements. This work is supported by the Netherlands Organization for Scientific Research (NWO), project number GO/13-01. The computations were carried out on the Dutch national supercomputer Cartesius, and we thank SURFSara (www.surfsara.nl) for their support. We would like to thank Twan van Noije and Tommi Bergman for kindly providing aerosol profiles for the initialisation of our simulations, Betty Croft for providing the data used for the scavenging look-up tables, and Chiel van Heerwaarden, Huug Ouwersloot and Xabier Pedruzo Bagazgoitia for their support with the DALES code.

References

Aan de Brugh, J. M. J., Ouwersloot, H. G., Vilà-Guerau de Arellano, J., and Krol, M. C.: A large-eddy simulation of the phase transition of ammonium nitrate in a convective boundary layer, J. Geophys. Res.: Atmos, 118, 826–836, https://doi.org/10.1002/jgrd.50161, 2013.

Albrecht, B. A.: Aerosols, Cloud Microphysics, and Fractional Cloudiness, Science, 245, 1227–1230, https://doi.org/10.1126/science.245.4923.1227, 1989.

Arabas, S., Jaruga, A., Pawlowska, H., and Grabowski, W. W.: libcloudph++ 1.0: a single-moment bulk, double-moment bulk, and particle-based warm-rain microphysics library in C++, Geosci. Model Dev., 8, 1677–1707, https://doi.org/10.5194/gmd-8-1677-2015, 2015.

Barbaro, E., Vilà-Guerau de Arellano, J., Krol, M. C., and Holtslag, A. A. M.: Impacts of Aerosol Shortwave Radiation Absorption on the Dynamics of an Idealized Convective Atmospheric Boundary Layer, Bound.-Lay. Meteorol., 148, 31–49, https://doi.org/10.1007/s10546-013-9800-7, 2013.

Barbaro, E., Arellano, J. V.-G., Ouwersloot, H. G., Schröter, J. S., Donovan, D. P., and Krol, M. C.: Aerosols in the convective boundary layer: Shortwave radiation effects on the coupled land-atmosphere system, J. Geophys. Res.: Atmos, 119, 5845–5863, https://doi.org/10.1002/2013JD021237, 2014.

Bergman et al., T.: Evaluation of a secondary organic aerosol scheme in TM5, in prep, 2019.

Boucher, O., Randall, D., Artaxo, P., Bretherton, C., Feingold, G., Forster, P., Kerminen, V.-M., Kondo, Y., Liao, H., Lohmann, U., Rasch, P., Satheesh, S., Sherwood, S., Stevens, B., and Zhang, X.: Clouds and Aerosols, book section 7, pp. 571 – 658, Cambridge University Press, Cambridge, United Kingdom and New York, NY, USA, https://doi.org/10.1017/CBO9781107415324.016, 2013.

Bretherton, C. S.: Insights into low-latitude cloud feedbacks from high-resolution models, Philos. T. Roy. Soc. A, 373, 20140 415, https://doi.org/10.1098/rsta.2014.0415, 2015.

Croft, B., Lohmann, U., Martin, R. V., Stier, P., Wurzler, S., Feichter, J., Posselt, R., and Ferrachat, S.: Aerosol size-dependent below-cloud scavenging by rain and snow in the ECHAM5-HAM, Atmos. Chem. Phys., 9, 4653–4675, https://doi.org/10.5194/acp-9-4653-2009, 2009.

Croft, B., Lohmann, U., Martin, R. V., Stier, P., Wurzler, S., Feichter, J., Hoose, C., Heikkilä, U., van Donkelaar, A., and Ferrachat, S.: Influences of in-cloud aerosol scavenging parameterizations on aerosol concentrations and wet deposition in ECHAM5-HAM, Atmos. Chem. Phys., 10, 1511–1543, https://doi.org/10.5194/acp-10-1511-2010, 2010.

de Bruine, M., Krol, M., van Noije, T., Le Sager, P., and Röckmann, T.: The impact of precipitation evaporation on the atmospheric aerosol distribution in EC-Earth v3.2.0, Geosci. Model Dev., 11, 1443–1465, https://doi.org/10.5194/gmd-11-1443-2018, 2018.

Derksen, J. W. B., Roelofs, G.-J. H., and Röckmann, T.: Influence of entrainment of CCN on microphysical properties of warm cumulus, Atmos. Chem. Phys., 9, 6005–6015, https://doi.org/10.5194/acp-9-6005-2009, 2009.

Fan, J., Wang, Y., Rosenfeld, D., and Liu, X.: Review of Aerosol-Cloud Interactions: Mechanisms, Significance, and Challenges, J. Atmos. Sci., 73, 4221–4252, https://doi.org/10.1175/JAS-D-16-0037.1, 2016.

Fan, J., Rosenfeld, D., Zhang, Y., Giangrande, S. E., Li, Z., Machado, L. A. T., Martin, S. T., Yang, Y., Wang, J., Artaxo, P., Barbosa, H. M. J., Braga, R. C., Comstock, J. M., Feng, Z., Gao, W., Gomes, H. B., Mei, F., Pöhlker, C., Pöhlker, M. L., Pöschl, U., and de Souza, R. A. F.: Substantial convection and precipitation enhancements by ultrafine aerosol particles, Science, 359, 411–418, https://doi.org/10.1126/science.aan8461, 2018.

Feingold, G. and Kreidenweis, S. M.: Cloud processing of aerosol as modeled by a large eddy simulation with coupled microphysics and aqueous chemistry, J. Geophys. Res.-Atmos., 107, AAC 6–1–AAC 6–15, https://doi.org/10.1029/2002JD002054, 2002.

Flamant, C., Knippertz, P., Fink, A. H., Akpo, A., Brooks, B., Chiu, C. J., Coe, H., Danuor, S., Evans, M., Jegede, O., Kalthoff, N., Konaré, A., Liousse, C., Lohou, F., Mari, C., Schlager, H., Schwarzenboeck, A., Adler, B., Amekudzi, L., Aryee, J., Ayoola, M., Batenburg, A. M., Bessardon, G., Borrmann, S., Brito, J., Bower, K., Burnet, F., Catoire, V., Colomb, A., Denjean, C., Fosu-Amankwah, K., Hill, P. G., Lee, J., Lothon, M., Maranan, M., Marsham, J., Meynadier, R., Ngamini, J.-B., Rosenberg, P., Sauer, D., Smith, V., Stratmann, G., Taylor, J. W., Voigt, C., and Yoboué, V.: The Dynamics–Aerosol–Chemistry–Cloud Interactions in West Africa Field Campaign: Overview and Research Highlights, B. Am. Meteorol. Soc., 99, 83–104, https://doi.org/10.1175/BAMS-D-16-0256.1, 2018.

Gong, W., Dastoor, A. P., Bouchet, V. S. B. S., Gong, S., Makar, P. A., Moran, M. D., Pabla, B., Menard, S., Crevier, L.-P., Cousineau, S., and Venkatesh, S.: Cloud processing of gases and aerosols in a regional air quality model (AURAMS), Atmos. Res., 82, 248 – 275, https://doi.org/10.1016/j.atmosres.2005.10.012, 14th International Conference on Clouds and Precipitation, 2006.

Grabowski, W. W., Morrison, H., Shima, S.-I., Abade, G. C., Dziekan, P., and Pawlowska, H.: Modeling of Cloud Microphysics: Can We Do Better?, B. Am. Meteorol. Soc., 100, 655–672, https://doi.org/10.1175/BAMS-D-18-0005.1, 2019.

Heikenfeld, M., White, B., Labbouz, L., and Stier, P.: Aerosol effects on deep convection: the propagation of aerosol perturbations through convective cloud microphysics, Atmos. Chem. Phys., 19, 2601–2627, https://doi.org/10.5194/acp-19-2601-2019, 2019.

Heus, T., van Heerwaarden, C. C., Jonker, H. J. J., Pier Siebesma, A., Axelsen, S., van den Dries, K., Geoffroy, O., Moene, A. F., Pino, D., de Roode, S. R., and Vilà-Guerau de Arellano, J.: Formulation of the Dutch Atmospheric Large-Eddy Simulation (DALES) and overview of its applications, Geosci. Model Dev., 3, 415–444, https://doi.org/10.5194/gmd-3-415-2010, 2010.

Hoffmann, F., Yamaguchi, T., and Feingold, G.: Inhomogeneous Mixing in Lagrangian Cloud Models: Effects on the Production of Precipitation Embryos, J. Atmos. Sci., 76, 113–133, https://doi.org/10.1175/JAS-D-18-0087.1, 2019.

Hundsdorfer, W., Koren, B., vanLoon, M., and Verwer, J.: A Positive Finite-Difference Advection Scheme, J. Comput. Phys., 117, 35 – 46, https://doi.org/https://doi.org/10.1006/jcph.1995.1042, 1995.

Jaruga, A. and Pawlowska, H.: libcloudph++ 2.0: aqueous-phase chemistry extension of the particle-based cloud microphysics scheme, Geosci. Model Dev., 11, 3623–3645, https://doi.org/10.5194/gmd-11-3623-2018, 2018.

Khain, A. P., Beheng, K. D., Heymsfield, A., Korolev, A., Krichak, S. O., Levin, Z., Pinsky, M., Phillips, V., Prabhakaran, T., Teller, A., van den Heever, S. C., and Yano, J.-I.: Representation of microphysical processes in cloud-resolving models: Spectral (bin) microphysics versus bulk parameterization, Rev. Geophys., 53, 247–322, https://doi.org/10.1002/2014RG000468, 2014RG000468, 2015.

Khairoutdinov, M. and Kogan, Y.: A New Cloud Physics Parameterization in a Large-Eddy Simulation Model of Marine Stratocumulus, Mon. Weather Rev., 128, 229–243, https://doi.org/10.1175/1520-0493(2000)128<0229:ANCPPI>2.0.CO;2, 2000.

Kokkola, H., Korhonen, H., Lehtinen, K. E. J., Makkonen, R., Asmi, A., Järvenoja, S., Anttila, T., Partanen, A.-I., Kulmala, M., Järvinen, H., Laaksonen, A., and Kerminen, V.-M.: SALSA; a Sectional Aerosol module for Large Scale Applications, Atmos. Chem. Phys., 8, 2469–2483, https://doi.org/10.5194/acp-8-2469-2008, 2008.

Koren, I., Martins, J. V., Remer, L. A., and Afargan, H.: Smoke Invigoration Versus Inhibition of Clouds over the Amazon, Science, 321, 946–949, https://doi.org/10.1126/science.1159185, 2008.

Kurppa, M., Hellsten, A., Roldin, P., Kokkola, H., Tonttila, J., Auvinen, M., Kent, C., Kumar, P., Maronga, B., and Järvi, L.: Implementation of the sectional aerosol module SALSA2.0 into the PALM model system 6.0: model development and first evaluation, Geosci. Model Dev., 12, 1403–1422, https://doi.org/10.5194/gmd-12-1403-2019, 2019.

Lebo, Z. J. and Seinfeld, J. H.: A continuous spectral aerosol-droplet microphysics model, Atmos. Chem. Phys., 11, 12 297–12 316, https://doi.org/10.5194/acp-11-12297-2011, 2011.

Martin, S. T., Artaxo, P., Machado, L., Manzi, A. O., Souza, R. A. F., Schumacher, C., Wang, J., Biscaro, T., Brito, J., Calheiros, A., Jardine, K., Medeiros, A., Portela, B., de Sá, S. S., Adachi, K., Aiken, A. C., Albrecht, R., Alexander, L., Andreae, M. O., Barbosa, H. M. J., Buseck, P., Chand, D., Comstock, J. M., Day, D. A., Dubey, M., Fan, J., Fast, J., Fisch, G., Fortner, E., Giangrande, S., Gilles, M., Goldstein, A. H., Guenther, A., Hubbe, J., Jensen, M., Jimenez, J. L., Keutsch, F. N., Kim, S., Kuang, C., Laskin, A., McKinney, K., Mei, F., Miller, M., Nascimento, R., Pauliquevis, T., Pekour, M., Peres, J., Petäjä, T., Pöhlker, C., Pöschl, U., Rizzo, L., Schmid, B., Shilling, J. E., Dias, M. A. S., Smith, J. N., Tomlinson, J. M., Tóta, J., and Wendisch, M.: The Green Ocean Amazon Experiment (GoAmazon2014/5) Observes Pollution Affecting Gases, Aerosols, Clouds, and Rainfall over the Rain Forest, B. Am. Meteorol. Soc., 98, 981–997, https://doi.org/10.1175/BAMS-D-15-00221.1, 2017.

Matheou, G., Chung, D., Nuijens, L., Stevens, B., and Teixeira, J.: On the Fidelity of Large-Eddy Simulation of Shallow Precipitating Cumulus Convection, Monthly Weather Review, 139, 2918–2939, https://doi.org/10.1175/2011MWR3599.1, 2011.

Mitra, S., Brinkmann, J., and Pruppacher, H.: A wind tunnel study on the drop-to-particle conversion, J. Aerosol Sci., 23, 245 – 256, https://doi.org/http://dx.doi.org/10.1016/0021-8502(92)90326-Q, 1992.

Ouwersloot, H. G., Moene, A. F., Attema, J. J., and de Arellano, J. V.-G.: Large-Eddy Simulation Comparison of Neutral Flow Over a Canopy: Sensitivities to Physical and Numerical Conditions, and Similarity to Other Representations, Bound.-Lay. Meteorol., 162, 71–89, https://doi.org/10.1007/s10546-016-0182-5, 2017.

Ovchinnikov, M. and Easter, R. C.: Modeling aerosol growth by aqueous chemistry in a nonprecipitating stratiform cloud, J. Geophys. Res.-Atmos., 115, https://doi.org/10.1029/2009JD012816, 2010.

Petters, M. D. and Kreidenweis, S. M.: A single parameter representation of hygroscopic growth and cloud condensation nucleus activity, Atmos. Chem. Phys., 7, 1961–1971, https://doi.org/10.5194/acp-7-1961-2007, 2007.

Pousse-Nottelmann, S., Zubler, E. M., and Lohmann, U.: Microphysical processing of aerosol particles in orographic clouds, AtJ. Atmos. Sci.mos. Chem. Phys., 15, 9217–9236, https://doi.org/10.5194/acp-15-9217-2015, 2015.

Pringle, K. J., Tost, H., Pozzer, A., Pöschl, U., and Lelieveld, J.: Global distribution of the effective aerosol hygroscopicity parameter for CCN activation, Atmos. Chem. Phys., 10, 5241–5255, https://doi.org/10.5194/acp-10-5241-2010, 2010.

Rauber, R. M., Stevens, B., Ochs, H. T., Knight, C., Albrecht, B. A., Blyth, A. M., Fairall, C. W., Jensen, J. B., Lasher-Trapp, S. G., Mayol-Bracero, O. L., Vali, G., Anderson, J. R., Baker, B. A., Bandy, A. R., Burnet, E., Brenguier, J.-L., Brewer, W. A., Brown, P. R. A., Chuang, R., Cotton, W. R., Di Girolamo, L., Geerts, B., Gerber, H., Göke, S., Gomes, L., Heikes, B. G., Hudson, J. G., Kollias, P., Lawson, R. R., Krueger, S. K., Lenschow, D. H., Nuijens, L., O'Sullivan, D. W., Rilling, R. A., Rogers, D. C., Siebesma, A. P., Snodgrass, E., Stith, J. L., Thornton, D. C., Tucker, S., Twohy, C. H., and Zuidema, P.: Rain in ShalloJ. Comput. Phys.w Cumulus Over the Ocean: The RICO Campaign, B. Am. Meteorol. Soc., 88, 1912–1928, https://doi.org/10.1175/BAMS-88-12-1912, 2007.

Riechelmann, T., Noh, Y., and Raasch, S.: A new method for large-eddy simulations of clouds with Lagrangian droplets including the effects of turbulent collision, New J. Phys., 14, 065 008, https://doi.org/10.1088/1367-2630/14/6/065008, 2012.

Roelofs, G. J. H.: Drop size dependent sulfate distribution in a growing cloud, J. Atmos. Chem., 14, 109–118, https://doi.org/10.1007/BF00115227, 1992.

Rosenfeld, D., Sherwood, S., Wood, R., and Donner, L.: Climate Effects of Aerosol-Cloud Interactions, Science, 343, 379–380, https://doi.org/10.1126/science.1247490, 2014.

Schneider, T., Teixeira, J., Bretherton, C. S., Brient, F., Pressel, K. G., Schär, C., and Siebesma, A. P.: Climate goals and computing the future of clouds, Nat. Clim. Change, 7, 3, https://doi.org/10.1038/nclimate3190, 2017.

Schultz, M. G., Stadtler, S., Schröder, S., Taraborrelli, D., Franco, B., Krefting, J., Henrot, A., Ferrachat, S., Lohmann, U., Neubauer, D., Siegenthaler-Le Drian, C., Wahl, S., Kokkola, H., Kühn, T., Rast, S., Schmidt, H., Stier, P., Kinnison, D., Tyndall, G. S., Orlando, J. J., and Wespes, C.: The chemistry–climate model ECHAM6.3-HAM2.3-MOZ1.0, Geosci. Model Dev., 11, 1695–1723, https://doi.org/10.5194/gmd-11-1695-2018, 2018.

Seifert, A.: On the Parameterization of Evaporation of Raindrops as Simulated by a One-Dimensional Rainshaft Model, J. Atmos. Sci., 65, 3608–3619, https://doi.org/10.1175/2008JAS2586.1, 2008.

Seifert, A. and Beheng, K. D.: A double-moment parameterization for simulating autoconversion, accretion and selfcollection, Atmospheric Research, 59-60, 265 – 281, https://doi.org/10.1016/S0169-8095(01)00126-0, 13th International Conference on Clouds and Precipitation, 2001.

Seifert, A. and Beheng, K. D.: A two-moment cloud microphysics parameterization for mixed-phase clouds. Part 1: Model description, Meteorol. Atmos. Phys., 92, 45–66, https://doi.org/10.1007/s00703-005-0112-4, 2006.

Seinfeld, J. H., Bretherton, C., Carslaw, K. S., Coe, H., DeMott, P. J., Dunlea, E. J., Feingold, G., Ghan, S., Guenther, A. B., Kahn, R., Kraucunas, I., Kreidenweis, S. M., Molina, M. J., Nenes, A., Penner, J. E., Prather, K. A., Ramanathan, V., Ramaswamy, V., Rasch, P. J., Ravishankara, A. R., Rosenfeld, D., Stephens, G., and Wood, R.: Improving our fundamental understanding of the role of aerosol-cloud interactions in the climate system, P. Natl. Acad. Sci. USA, 113, 5781–5790, https://doi.org/10.1073/pnas.1514043113, 2016.

Sommeria, G. and Deardorff, J. W.: Subgrid-Scale Condensation in Models of Nonprecipitating Clouds, J. Atmos. Sci., 34, 344–355, https://doi.org/10.1175/1520-0469(1977)034<0344:SSCIMO>2.0.CO;2, 1977.

Stevens, B. and Feingold, G.: Untangling aerosol effects on clouds and precipitation in a buffered system, Nature, 461, 607–613, https://doi.org/10.1038/nature08281, 2009.

Stevens, B. and Seifert, A.: Understanding macrophysical outcomes of microphysical choices in simulations of shallow cumulus convection, J. Meteorol. Soc. Jap. Ser. II, 86A, 143–162, https://doi.org/10.2151/jmsj.86A.143, 2008.

Tonttila, J., Maalick, Z., Raatikainen, T., Kokkola, H., Kühn, T., and Romakkaniemi, S.: UCLALES–SALSA v1.0: a large-eddy model with interactive sectional microphysics for aerosol, clouds and precipitation, Geosci. Model Dev., 10, 169–188, https://doi.org/10.5194/gmd-10-169-2017, 2017.

Twomey, S.: The Influence of Pollution on the Shortwave Albedo of Clouds, J. Atmos. Sci., 34, 1149–1152, https://doi.org/10.1175/1520-0469(1977)034<1149:TIOPOT>2.0.CO;2, 1977.

van Noije, T. P. C., Le Sager, P., Segers, A. J., van Velthoven, P. F. J., Krol, M. C., Hazeleger, W., Williams, A. G., and Chambers, S. D.: Simulation of tropospheric chemistry and aerosols with the climate model EC-Earth, Geosci. Model Dev., 7, 2435–2475, https://doi.org/10.5194/gmd-7-2435-2014, 2014.

vanZanten, M. C., Stevens, B., Nuijens, L., Siebesma, A. P., Ackerman, A. S., Burnet, F., Cheng, A., Couvreux, F., Jiang, H., Khairoutdinov, M., Kogan, Y., Lewellen, D. C., Mechem, D., Nakamura, K., Noda, A., Shipway, B. J., Slawinska, J., Wang, S., and Wyszogrodzki, A.: Controls on precipitation and cloudiness in simulations of trade-wind cumulus as observed during RICO, Journal of Advances in Modeling Earth Systems, 3, https://doi.org/10.1029/2011MS000056, 2011.

Vignati, E., Wilson, J., and Stier, P.: M7: An efficient size-resolved aerosol microphysics module for large-scale aerosol transport models, J. Geophys. Res. Atmos., 109, https://doi.org/10.1029/2003JD004485, 2004.

Vilà-Guerau de Arellano, J., Patton, E. G., Karl, T., van den Dries, K., Barth, M. C., and Orlando, J. J.: The role of boundary layer dynamics on the diurnal evolution of isoprene and the hydroxyl radical over tropical forests, J. Geophys. Res.: Atmos, 116, https://doi.org/10.1029/2010JD014857, 2011.

Vilà-Guerau de Arellano, J., Ouwersloot, H. G., Baldocchi, D., and Jacobs, C. M. J.: Shallow cumulus rooted in photosynthesis, Geophysical Research Letters, 41, 1796–1802, https://doi.org/10.1002/2014GL059279, 2014.

Wehner, B., Werner, F., Ditas, F., Shaw, R. A., Kulmala, M., and Siebert, H.: Observations of new particle formation in enhanced UV irradiance zones near cumulus clouds, Atmos. Chem. Phys., 15, 11 701–11 711, https://doi.org/10.5194/acp-15-11701-2015, 2015.

Wesseling, P.: von Neumann stability conditions for the convection-diffusion eqation, IMA J. Numer. Anal., 16, 583–598, https://doi.org/10.1093/imanum/16.4.583, 1996.

Wicker, L. J. and Skamarock, W. C.: Time-Splitting Methods for Elastic Models Using Forward Time Schemes, Mon. Weather Rev., 130, 2088–2097, https://doi.org/10.1175/1520-0493(2002)130<2088:TSMFEM>2.0.CO;2, 2002.

Williams, J. E., Boersma, K. F., Le Sager, P., and Verstraeten, W. W.: The high-resolution version of TM5-MP for optimized satellite retrievals: description and validation, Geosci. Model Dev., 10, 721–750, https://doi.org/10.5194/gmd-10-721-2017, 2017.